UNIVERSITATEA DE STAT „ALECU RUSSO” DIN BĂLŢI

ISSN 1857-0437

FIZICĂ ŞI TEHNICĂ:
procese, modele, experimente

Revistă ştiinţifică a profilului de cercetare
„Fizica şi tehnologia mediilor materiale”

2
2013

Bălţi

Fondatorul: Universitatea de Stat „Alecu Russo” din Bălţi

Anul fondării: 2006

Colegiul de redacţie:
Pavel Topală, dr. hab., prof., **redactor-şef**, Universitatea de Stat „Alecu Russo” din Bălţi, Republica Moldova
Ion Tighineanu, academician, Academia de Ştiinţe a Moldovei
Valeriu Canţer, academician, Academia de Ştiinţe a Moldovei
Leonid Culiuc, academician, Academia de Ştiinţe a Moldovei
Alexandr Dikusar, membru corespondent, Academia de Ştiinţe a Moldovei
Petru Stoicev, dr. hab., prof., Universitatea Tehnică a Moldovei
Alexandr Mihailov, dr. hab., prof., Universitatea Tehnică din Doneţk, Ukraina
Nicolai Zaicenco, dr. hab., prof., Academia Naţională de construcţie şi arhitectură din Donbas, Ukraina
Dumitru Nedelcu**,** dr. ing., prof., Universitatea Tehnică ”Gheorghe Asachi”, Iaşi, România
Makio Naito, dr. ing., prof., Universitatea din Osaka, Japonia
Alexandar Makedonski**,** dr. ing., prof., Universitatea Technică din Sofia, Bulgaria
Andrzej Wrobel, dr. ing., Universitatea Tehnologică din Silezia, Gliwice, Polonia
Valeriu Ureadov, dr. hab., Institutul de Radiofizică, Nijnii Novgorod, Rusia
Laurenţiu Slătineanu, dr. ing., prof., Universitatea Tehnică „Gheorghe Asachi”, Iaşi, România
Gheorghe Popa, dr., prof., Universitatea „Alexandru Ioan Cuza”, Iaşi, România
Vasile Şaragov, dr. hab., conf., Universitatea de Stat „Alecu Russo” din Bălţi, Republica Moldova
Valeriu Dulgheru, dr. hab., prof., Universitatea Tehnică a Moldovei
Alexandru Balanici, dr., conf., Universitatea de Stat „Alecu Russo” din Bălţi, Republica Moldova
Valeriu Guţan, dr., conf., Universitatea de Stat „Alecu Russo” din Bălţi, Republica Moldova
Alexandr Ojegov, dr., lect., **secretar ştiinţific**, Universitatea de Stat „Alecu Russo” din Bălţi, Republica Moldova

Tehnoredactare:
Alexandr Ojegov, dr., lect., Universitatea de Stat „Alecu Russo” din Bălţi

Design şi aspectul paginii de titlu:
Alexandr Ojegov, dr., lect., Universitatea de Stat „Alecu Russo” din Bălţi

Redactori:
Ala Sainenco, dr., conf., Universitatea de Stat „Alecu Russo” din Bălţi
Elena Sirota, dr., conf., Universitatea de Stat „Alecu Russo” din Bălţi
Iulia Ignatiuc, dr., conf., Universitatea de Stat „Alecu Russo” din Bălţi

Adresa redacţiei: Universitatea de Stat „Alecu Russo” din Bălţi,
str. Puşkin 38, 3100, Bălţi, Republica Moldova
Tel.: (231)52368, fax: (231)52439
E-mail: libruniv.usarb.md/publicatie/fizteh.htm

Tiparul: Tipografia Indigou Color
© Universitatea de Stat „Alecu Russo” din Bălţi
Presa universitară bălţeană, 2013

ISSN 1857-0437

CUPRINS

CONTENTS

CZU 620.9 (075.8)

STUDY OF PHYSICO-MECHANICAL PROPERTIES OF COMPOSITE IRON-NICKEL COATINGS AND THEIR IMPACT ON THERMAL RESISTANCE OF BOUNDARY LAYERS OF LUBRICANTS

Javgureanu V.*, Gordelenco P.
Universitatea Tehnică a Moldovei, bd. Ştefan cel Mare, 168, MD-2004, Chişinău, Republica Moldova
*e-mail: v_javgureanu@yahoo.com

Articolul prezintă studiul proprietăţilor fizico-mecanice (Ae, Ap, A, he, Hh, Hd, P) şi rezistenţei termice (Tcr) a straturilor de graniţă de ulei de lubrifiere M12B în timpul frecării acoperirilor compozite de fier-nichel. S-a stabilit experimental că acoperirile de fier-nichel cu proprietăţi fizico-mecanice sporite (Ae, Ap, A, he, Hh, Hd, P) contribuie la sporire a rezistenţei termice (Tcr) a straturilor de graniţă de ulei de lubrifiere M12B.
Cuvinte-cheie: acoperire fier-nichel, lubrifiere, straturi, proprietăţi fizico-mecanice, rezistenţă termică, frecare.

The paper presents the study of physico-mechanical properties (Ae, Ap, A, he, Hh, Hd, P) and thermal resistance (Tcr) of boundary lubricating oil layers M12B during the rubbing of composite iron-nickel coatings. It was experimentally established that iron-nickel coatings with higher physical and mechanical properties (Ae, Ap, A, he, Hh, Hd, P) contribute to the increase of thermal resistance (Tcr) of boundary lubricating oil layers M12B.
Keywords: iron-nickel coatings, lubricating, layers, physic-mechanical properties, thermal resistance, rubbing.

1. INTRODUCTION

The relevance of research and testing of physical and mechanical properties of materials at the surface and in the surface layers due to the fact that the contact interaction and contact deformation associated with nearly all modern methods of treatment, hardening and metal compounds, but also service properties of metals in terms of friction, fatigue, seizure and wear.

One of their methods of testing the surface properties of materials-test macro hardness.

2. GENERAL INFORMATION

In recent years developed methods and devices, allowing obtaining a wealth of information about the properties of materials at macro indentation. Material test method allows macro indentation measure several important parameters characterizing the physical and mechanical properties of composite plating, traditional and new, obtained only when these tests. The method of investigation of physical and mechanical properties of the coating is based on recording the kinetic diagram of a spherical diamond indenter indentation. As the spherical diamond indenter was used synthetic diamond sphere with radius equal to 1 mm.

Subjected to testing composite iron-coating thickness of 0.5 mm, the diameter of the sample in this case is 30 mm.

Test method for macrohardness allows testing of the wide application of materials with a thickness of 1 mm or more. Thus it is possible to determine not only the strength characteristics of the material but also its elastoplastic properties.

Many researchers have studied the shape of the plastically deformable deformation zones, and in the nature of a screen where the fingerprint shown that the boundary area of plastically deformable nature of the deformation and the diameter d a fingerprint similar in shape to the part of a sphere for both metals and polymers.

We studied the deformation of deep and surface layers of materials under the indenter by applying a grid meridian section in the plane of the sample. We prove that the maximal deformation axis indentation depth of approximately half the radius of the print at the point of maximum shear stress. On the surface indentation deformation grow from the center of the contour near the circuit decreases and beyond change direction. Inverting the direction of deformation occurs due to the fact that the printout at some

distance underneath the material undergoes axial compression and broadening in the radial direction.

This paper presents the study of physical and mechanical properties of Fe-Ni composite coatings by indentation spherical diamond indenter.

Experimentally determined: elastoplastic characteristics (**he**; **hp**, **h**); work spent on elastic (**Ay**), plastic (**Ap**), and the total deformation (**A**); unrestored (**Hh**) and dynamic (**Hd**) hardness, indentation load on a spherical diamond indenter (**P**), the volume of elastic (**Ve**), a plastic (**Vp**) and the total (**V**) of a deformable composite material of iron-nickel coatings produced from the electrolyte 4 [2]. The above characteristics were determined at the facility for the study of the hardness of materials in macro volume equipped with an inductive sensor and a differential amplifier to record chart indentation spherical diamond indenter and indentation recovery after unloading.

The dynamic hardness (**Hd**) was determined as the ratio of the total of (**A**) consumed for the total deformation of the material (**V**) the volume of deformable material all studied Fe-Ni coating. Important indicators in assessing the anti-friction properties of bearing materials is their ability to provide at the operating temperatures of the bearing and lubrication conditions instantaneous coefficient of friction and cause seizure and seizure in the destruction of the lubricating layer separating the friction surface [2]. For protection from seizure is important to assess the maximum allowable friction conditions, depending on the combination of the properties of materials and lubricants [2]. Studies have shown that the destruction of the boundary layer for the material and lubrication occurs when the contact zone a certain critical temperature constant for the combination of such material and grease. Thermal resistance of the boundary lubricant layer is estimated complex material and lubricating oil. These properties can be attributed to the ability of the interacting surfaces gripe adhesive bond with oil film on the surface, the ability to recover these bonds at fracture oxidability friction surfaces as well as the quality of the oxidized films [2].

Defined critical temperature boundary layer lubricating in friction materials used friction machine **MAST - 1** operates as a cone - ring sample [2]. On a conical pattern with an apex angle of 110°±1° composite iron-deposited coatings, which have been processed by grinding and polishing. Working on an annular surface sample was created as a result of pressing the same geometry of the cone on the press under load -dependent plasticity. In the case of low ductility materials (iron) treatment by a special ring shaped cutters mounted on the bottom hole sample. With a width of 0.2 mm was provided by the belt contact geometry, which is close to linear.

The magnitude of unit loads at the site of contact for selected sample sizes and design features of the machine **MAST–1** varied from $25\cdot10^{-3}$ N/m^2. The speed of rotation of the upper sample is 1 rot/min, which corresponds to $0.42\cdot10^{3}$ sliding speed for indicating the size of the sample. Bulk oil temperature was varied from 20 to 400°C.

Before testing, the samples were kept in the oil for one hour to form on their surface oriented layers oil. Burnishing the samples was carried out under a load of $10\cdot10^{-3} \div 15\cdot10^{-3}$N/m^2. On completion of the run-in to establish the position of judge of the pen recorder. Counter body was made of alloyed cast iron following chemical composition:
C_{total}=3.75%; $C_{binding}$=0.75%; Si=2.45%; Mn=0.65%; P=0.15%; Cr=0.25%; Ni=0.11%; Cu=0.75%; S=0.11%; Mo=0.4%.

Alloy cast iron made factory - rings made from the same cast. Proved that by varying the density of only **Dκ** and electrolyte temperature can change physics - the mechanical properties of iron-nickel coatings (**Ae**, **Ap**, **A**, **Hh**, **Hd**, **P**).

3. DISCUSSION OF EXPERIMENTAL RESEARCH

Studies have shown that the investigated characteristics of composite iron-nickel coatings vary with the conditions of their receipt ($\mathbf{D_K}$, **T**).

With increasing current density (**D_k**) of from 5 to 80 ($\times 10^{-4}$ kA/m^2) at a constant temperature of electrolysis (40 ^{0}C), the elastic indentation depth (**he**) and the amount of elastic indentation of the coating material (**Vy**) increases, respectively, from 1.34 to 1.35 (micrometers), and from 40.34 to 57.17×10^{-7} (mm^3) Table 1. Dependence unreduced hardness (**Hh**), dynamic hardness (**Hd**), the load on the indenter (**P**) and the work expended on the elastic deformation of coatings (**Ae**) are extreme.

With increasing current density from 5 to 50 ($\times 10^{-4}$ kA/m^2), hardness (**Hh**) increased from 3630 to 4470 (N/mm^2), the dynamic hardness (**Hd**) increased from 2422 to 2890 (N/mm^2), the load on a spherical diamond indenter increased from 45.6 to 56.1 (H), and the work spent on the elastic deformation Fe-Ni composite coatings (Ae) increased from 17.23×10^{-3} to 23.56×10^{-3} (N·mm). With a further increase in current density from 50 to 80 ($\times 10^{-4}$ kA/m^2), the hardness (**Hh**) decreased from 4470 to 3320 (N/mm^2), the dynamic hardness (**Hd**) decreased from 2980 to 2215 (N/mm^2), the force of the diamond spherical indenter (P) decreased from 56.1 to 41.7 (N) and the work spent on the elastic deformation (**Ay**) Fe-Ni composite coatings decreased from 23.56×10^{-3} to 15.77×10^{-3} (N/mm).

Extreme hardness (**Hh**), a dynamic hardness (**Hd**), load on a spherical diamond indenter (**P**) and the work consumed by the elastic deformation of Fe-Ni composite coatings coincide with the existing guidelines for the choice of Electrolysis conditions for optimum Fe-Ni coating from the standpoint their wear resistance.

Table 1

Elastic properties of hardness and Fe-Ni composite coatings

Electrolysis conditions		Hh, N/mm^2 (h=2μm)	Hd, N/mm^2	P, N	***Elastic properties of the Fe-Ni coating***		
Dk, $\times10^{-4}$ kA/m^2	T,^{0}C				he, μm	Ap, N·mm	Ve, $\times10^{-7}$ mm^3
5	40	3630	2422	45.6	1.134	0.01723	40.34
10	40	3670	2449	46.1	1.150	0.01767	41.47
20	40	3800	2534	47.7	1.172	0.01863	43.11
30	40	3980	2656	50.0	1.210	0.02017	45.93
40	40	4120	2746	51.7	1.240	0.02137	48.23
50	40	4470	2980	56.1	1.26	0.02356	49.80
60	40	4020	2683	50.5	1.28	0.02020	51.40
80	40	3320	2215	41.7	1.35	0.01577	57.17

Table 2

Plastic properties and hardness Fe-Ni composite coatings

Electrolysis conditions		Hh, N/mm^2 (h=2 μm)	Hd, N/mm^2	P, N	***Plastic properties of Fe-Ni coating***		
Dκ, $\times10^{-4}$ kA/m^2	T,^{0}C				hp, μm	Ap, N·mm	Vp, $\times10^{-7}$ mm^3
5	40	3630	2422	45.6	0.8660	0.01316	23.57
10	40	3670	2449	46.1	0.8500	0.01351	22.67
20	40	3800	2534	47.7	0.8280	0.01357	21.50
30	40	3980	2656	50.0	0.7900	0.01361	19.56
40	40	4120	2746	51.7	0.7600	0.01369	18.11
50	40	4470	2980	56.1	0.7400	0.01384	17.17
60	40	4020	2683	50.5	0.7200	0.01212	16.26
80	40	3320	2215	41.7	0.6500	0.00904	13.25

Table 3

Elastic-plastic properties and hardness of Fe-Ni composite coatings

Electrolysis conditions		Hh, N/mm^2 (h=2 μm)	Hd, N/mm^2	P, N	***Elastoplastic properties***		
Dκ, $\times10^{-4}$ kA/m^2	T, ^0C				h, μm	A, N·mm	V, $\times10^{-7}$ mm^3
5	40	3630	2422	45.6	2.0	0.03040	125.51
10	40	3670	2449	46.1	2.0	0.03073	125.51
20	40	3800	2534	47.7	2.0	0.03180	125.51
30	40	3980	2656	50.0	2.0	0.0333	125.51
40	40	4120	2746	51.7	2.0	0.0347	125.51
50	40	4470	2980	56.1	2.0	0.03740	125.51
60	40	4020	2683	50.5	2.0	0.0337	125.51
80	40	3320	2215	41.7	2.0	0.02780	125.51

With increasing current density (D_k) - table 2, from 5 to 40 ($\times10^4$ kA/m^2) at a constant temperature of electrolysis (40 ^0C) of the plastic indentation depth (**hp**) and the volume of plastic indentation test material (**Vp**), respectively decrease from 0.866 to 0.740 (micrometers), and from 23.57×10^{-7} to 17.17×10^{-7} (mm^3). With increasing density of 5 to 50 ($\times10^{-4}$ kA/m^2) at a constant temperature of electrolysis (40^0C) hardness (**Hh**), a dynamic hardness (**Hd**) indentation load (P) has increased as in the previous case (Table 1) and the work expended in plastic deformation (**Ap**) Fe-Ni composite coatings increased from 13.16×10^{-3} to 13.84×10^{-3} (N·mm).

With a further increase in current density (D_k) at constant electrolysis temperature (40 ^0C) of 50 to 80 ($\times10^{-4}$ kA/m^2) hardness (**Hh**), a dynamic hardness (**Hd**), indentation load (**P**) and reduced as in the previous case (table 1), and the work expended in plastic deformation of Fe-Ni composite coatings decreased from 13.84×10^{-3} to 9.04×10^{-3} (N·mm).

And in this case, the extreme hardness (**Hh**), dynamic hardness (**Hd**), indentation load (**P**) and the work expended in plastic deformation (**Ap**) Fe-Ni composite coatings coincide with existing recommendations for choosing electrolysis conditions to obtain optimal properties Fe- Ni coatings in terms of wear resistance [2].

With increasing current density ($\mathbf{D_k}$) in table 3, from 5 to 80 ($\times10^{-4}$ kA/m^2) (at a constant temperature of electrolysis (40^0C) total indentation depth (h) and the total amount of material pressed into coatings (V) are constant, and are respectively 2.0 (μm) and 125.51×10^{-7} (mm^3).

With increasing current density ($\mathbf{D_k}$) from 5 to 50 ($\times10^{-4}$ kA/m^2) at a constant temperature of electrolysis (40^0C) hardness (**Hh**), a dynamic hardness (**Hd**) indentation load (P) increases in both the previous cases (tables 1 and 2) and consumed by the deformation work Fe-Ni composite coatings (a) is increased from 30.4×10^{-3} to 37.4×10^{-3} (N·mm). With a further increase in current density ($\mathbf{D_k}$), electrolysis at a constant temperature (40 ^0C) of 50 to 80 ($\times10^{-4}$ kA/m^2) Hardness (Hh), a dynamic hardness (**Hd**), at indentation load spherical diamond indenter (**P**) decreases both preceding case (table 1 and 2) and total work expended by deforming Fe-Ni composite coatings decreased from 37.4×10^{-3} to 27.8×10^{-3} (N·mm).

And in this case, the experimental values of hardness (**Hh**), dynamic hardness (**Hd**), indentation load spherical diamond indenter (P) and the work spent on the total deformation of Fe-Ni composite coatings (**A**) coincide with current recommendations for choosing electrolysis conditions for optimum properties of Fe-Ni composite coatings in terms of wear resistance.

With increasing temperature electrolysis (**T**) for obtaining Fe-Ni composite coatings (Table 4) of 20 to 60^0C (at $Dk=50\times10^{-4}$ kA/m^2), the elastic component of the depth of the indentation (**hu**) decreased from 1.52 to 1.028 μm, print volume (**Ve**) also decreased

from 72.5×10^{-7} to 33.15×10^{-7} mm^3. With increasing temperature electrolysis from 20 to 40^0C, hardness (**Hh**) has increased from 3320 to 4470 (N/mm^2), dynamic hardness (**Hd**) increased from 2215 to 2980 N/mm^2, indentation load on the diamond spherical indenter (**P**) increased from 41.7 to 56.1 (N), the work spent on the elastic deformation of Fe-Ni composite coatings (**Ae**) increased from 21.13×10^{-3} to 23.56×10^{-3} (H·mm), and the volume of print on elastic deformation of coatings (**Ve**) decreased from 72.5×10^{-7} to 49.8×10^{-7} (mm^3).

Table 4

Elastic properties of hardness and Fe-Ni coating.

Electrolysis conditions		Hh, N/mm^2 (h=2 μm)	Hd, N/mm^2	P, N	***Elastic properties of the Fe-Ni coating***		
Dk, $x10^{-4}$ kA/m^2	T, ^{0}C				he, μm	Ae N·mm	Ve, $\times10^{-7}$ mm^3
50	20	3320	2215	41.7	1.52	0.02113	72.50
50	40	4470	2980	56.1	1.26	0.02356	49.80
50	60	3630	2422	45.6	1.028	0.01563	33.15

With further increase of the electrolysis temperature (**T**) of 40 to 60^0C, a hardness (**Hh**) was reduced from 4470 to 3630 (N/mm^2), the dynamic hardness (**Hd**) decreased from 2980 to 2422 (N/mm^2), the force on a spherical diamond indenter (**P**) decreased from 56.1 to 45.6 (H**)**, and the work spent on the elastic deformation (**Ae**) Fe-Ni composite coatings decreased from 23.56×10^3 do 15.63×10^{-3} (N·mm).

In this case, the experimental values of hardness (**Hh**), a dynamic hardness (**Hd**), at indentation load spherical diamond indenter (**P**), the work expended in elastic deformation Fe-Ni composite coating (**Ae**), depending on the electrolysis temperature (**T**) at constant current density (**Dk**=50×10^{-4} kA/m^2) coincide with current recommendations for choosing electrolysis conditions to obtain optimal properties of Fe-Ni composite coating with the point of view of their optimum wear resistance [2].

With increasing temperature electrolysis (**T**), upon receipt of Fe-Ni composite coating (Table 5) of 20 to 60^0C (when **Dk**=50×10^{-4} kA/m^2) plastic components.

Table 5

Plastic properties and hardness Fe-Ni composite coating

Electrolysis conditions		Hh, N/mm^2 (h=2μm)	Hd, N/mm^2	P, N	***Plastic properties***		
Dk, kA/m^2	T, ^{0}C				hp, μm	Ap, N·mm	Vp, $\times10^{-7}$ mm^3
50	20	3320	2215	41.7	0.480	0.00667	7.22
50	40	4470	2980	56.1	0.740	0.01384	17.17
50	60	3630	2422	45.6	0.972	0.01877	29.64

Table 6

Elastoplastic properties hardness and Fe-Ni composite coatings

Electrolysis conditions		Hh, N/mm^2 (h=2μm)	Hd, N/mm^2	P, N	***Elastoplastic properties***		
Dk, kA/m^2	T, ^{0}C				h, μm	A, N·mm	V, $\times10^{-7}$ mm^3
50	20	3320	2215	41.7	2.0	0.02780	125.51
50	40	4470	2980	56.1	2.0	0.03740	125.51
50	60	3630	2422	45.6	2.0	0.03040	125.51

Extrusion depth (hp) increased from 0.48 to 0.972 (μm) and the volume of print for plastic indentation (**Vp**) increased from 7.22×10^{-3} to 29.64×10^{-3} (mm^3).

With increasing temperature electrolysis from 20 to 40 hardness (**Hh**), dynamic hardness (**Hd**), indentation load on the diamond spherical indenter (P) increased in value as in the previous case (table 4), and the work expended in plastic deformation (**Ap**) is Fe-Ni composite coatings increased from 6.67×10^{-3} to 13.84×10^{-3} (N·mm).

With further increase in temperature electrolysis (**T**) from 40 to 60^0C hardness (**Hh**) dynamic hardness (**Hd**), indentation load on the diamond spherical indenter (**P**) decreased in value as in the previous case (table 4), and the work expended in plastic deformation of Fe-Ni composite coatings (**Ap**) decreased from 13.84×10^{-3} to 13.77×10^{-3} (N·mm).

With increasing temperature electrolysis (**T**) of 20 to 60^0C in the preparation of Fe-Ni composite coating at a constant current density ($Dk=50\times10^{-4}$ kA/m^2), the total indentation depth (h) of the diamond and the amount of spherical indenter indentation (**P**) under elastoplastic indentations are constants and are, respectively, 2.0 (micrometers) and 125.51×10^{-3} (mm^3) table 6.

With increasing temperature electrolysis (**T**) of 20 to 40^0C at a constant current density ($Dk=50\times10^{-4}$ kA/m^2) hardness (**Hh**), a dynamic hardness (**Hd**), at indentation load spherical diamond indenter (**P**), increasing meaningfully as in the previous case (Table 4 and 5) and the work spent on elastoplastic indentations Fe-Ni composite coatings with indentations increased from 27.8×10^{-3} to 37.4×10^{-3} (N·mm). With further increase in temperature electrolysis (**T**) from 40 to 60^0C (at $Dk=50\times10^{-4}$ kA/m^2), hardness (**Hh**), dynamic hardness (**Hd**), indentation load on the diamond spherical indenter (**P**) decreased in value as in the previous cases (table 4 and 5), and the work spent on the elastic-plastic deformation.

Elastoplastic properties and hardness of Fe-Ni composite coatings decreased from 37.4×10^{-3} to 30.4×10^{-3} (N·mm). As in the previous cases (see table 4 and 5) with the increase in the electrolysis temperature (**T**), hardness (**Hh**), a dynamic hardness (**Hh**), load on a spherical indentation diamond indenter (**P**) and the work consumed by elastoplastic deformation of Fe-Ni composite coatings is experimental.

To study the thermal stability of the boundary layers in the test sediments having different physical and mechanical properties derived from one electrolyte, experiments were conducted with iron-nickel alloy rubbing against alloyed iron in the presence of oil **M12B** (tables 1 and 2).

Investigated iron-nickel coatings produced at a current density of 20×10^{-4}, 50×10^{-4}, and 80×10^{-4} kA/m^2, electrolysis temperature of 20, 40 and 60 °C and $P_H=0.8\div1.0$.

Table 7

Physical and mechanical properties of iron-nickel coatings and thermal resistance of the boundary lubricating oil layers M12B in friction coatings alloyed iron

Electrolysis conditions		***Work expended on the deformation of coatings***			H_h N/mm^2 (h=2μm)	H_d N/mm^2	P, N	$T_{cr,}$ ˚C
Dκ, $\times10^{-4}$ kA/m^2	T, ˚C	A_y N·mm	A_p N·mm	A N·mm				
5	40	0.0172	0.0132	0.0304	3630	2422	45.6	---
10	40	0.0127	0.0135	0.0312	3670	2449	46.1	---
20	40	0.0186	0.0132	0.0318	3800	2534	47.7	100
30	40	0.0202	0.0132	0.0334	3980	2556	50.0	---
40	40	0.0214	0.0132	0.0346	4120	2746	51.7	---
50	40	0.0235	0.0134	0.0373	4470	2980	56.1	220
60	40	0.0202	0.0121	0.0323	4020	2683	50.5	---
80	40	0.0188	0.0090	0.0278	3320	2215	41.7	100

Table 8

Physical and mechanical properties of iron-nickel coatings and thermal resistance of the boundary lubricating oil layers M12B in friction coatings alloyed iron.

Electrolysis conditions		***Work expended on the deformation of coatings***			H_h N/mm^2 (h=2μm)	H_d N/mm^2	P, N	T_{cr}, ˚C
Dк, $\times10^{-4}$, kA/m^2	T, ˚C	A_y N·mm	A_p N·mm	A N·mm				
50	20	0.42011	0.0067	0.0278	3320	2215	41.7	140
50	40	0.0235	0.0148	0.0373	4470	2980	56.1	220
50	60	0.0156	0.0138	0.0294	3630	2422	45.6	170

It was established experimentally that the friction alloy iron-nickel alloy cast iron for selected coatings are characterized by the conditions under which the transition occurs from smooth sliding to interrupt (the critical temperature). The cover with less physical and mechanical properties (**Ay**, **Ap**, A, **Hh**, **Hd**, **P**, table 7 and 8), the critical condition occurs at lower temperatures, oil **M12B**.

Thus, when the friction on the alloyed iron from iron-nickel alloy, received at a current density of 20×10^{-4} and 80×10^{-4} kA/m^2 (at T=40 °C), respectively, the critical condition occurs at an oil temperature of 10 and 100 °C. while coating obtained at a current density of 50×10^{-4} kA/m^2 (at T=40 °C), promote the preservation of the boundary layer lubrication to 220 °C.

Rubbing against iron-alloyed iron in sediments obtained from (a current density of 50×10^{-4} kA/m^2) temperature electrolysis 20, 40, 60 °C also comes the transition from smooth sliding to intermittent. We cover lower physical and mechanical characteristics (**Ae**, **Ap**, **A**, **Hh**, **Hd**, **P**), the critical condition occurs at lower temperatures, oil M12B (table 8).

Thus, when the friction on the cast iron alloyed coating obtained from electrolysis at temperatures of 20 and 60 °C (at **Dk**=50×10^{-4} kA/m^2), the critical state occurs at the oil temperature respectively of 140 and 170 °C, while the temperature of the coating obtained by electrolysis 40 °C (with **Dk**=50×10^{-4} kA/m^2), contribute to the preservation of boundary lubrication

Physical and mechanical properties of iron- nickel coatings and thermal resistance of the boundary lubricating oil layers **M12B** at friction coatings alloyed iron.

The experiments showed that, ceteris paribus, iron -nickel coatings with higher physical and mechanical properties (**Ae**, **Ap**, **A**, **Hh**, **Hd**, **P**) contribute to the thermal resistance of the boundary lubricant layers and improved their anti-friction properties. These models are stored, regardless of the type of material used rider and lubrication [2].

4. CONCLUSION

Found unrestored hardness (**Hh**) and the dynamic hardness (**Hd**), the work spent on elastoplastic deformation (A) have the extreme nature of changes in the conditions of electrolysis (**Dk**, **T**) for the study of iron-nickel composite coatings.

Experimental values not restored hardness (**Hh**), dynamic hardness (**Hd**), indentation load diamond spherical indenter (**P**), the work spent on plastic (**Ap**) and elastic-plastic deformation (**A**) coincides with our earlier recommendations for iron-nickel composite coatings with the point of view of their optimum durability.

Physical and mechanical characteristics (**Hh**, **Hd**, **P**, **Ap**) iron-nickel composite coatings have a good correlation with temperature resistance

Boundary lubricating oil layers **M12B** rubbing against alloyed iron.

BIBLIOGRAPHY

1. Булычев С. И., Алехин В. Н. Испытание материалов непрерывным вдавливанием индентора. Москва, Машиностроение, 1990, 224с.
2. Гологан В. Ф., Аждер В. В., Жавгуряну В. Н. Повышение долговечности

деталей машин износостойкими покрытиями. Кишинев, Изд-во Штиинца, 1979, 112 с.
3. Javgureanu V., Ajder V., Ceban V., Pavlova . The correlation of restored and unrestored microhardness of. Wear-proof iron plating. Conferinţă Ştiinţifică Internaţională TMCR. Chişinău, 2003, pp.412-415.
4. Javgureanu, V.; Gordelenco, P.; Elita, M. The work of deforming wear -proof iron-nikel plating in microsquelging. The Annals of University "Dunărea de Jos" of Galaţi, Fascicle VIII, 2004, Tribology, Romania, pp. 65-68.
5. Javgureanu, V.; Gordelenco, P.; Elita, M. Relationship of the restored and unrestored microharedbess of the cromium coating. The Annals of University "Dunărea de Jos" of Galaţi, Fascicle VIII, 2004 Tribology, Romania, pp. 48-51.
6. Javgureanu, V.; Gordelenco, P.; Elita, M. Le rapport de la microdurete restauree et non restauree des convertures de crome. Conferinţă Ştiinţifică Internaţională TMCR, Chişinău, 2005, pp. 166-169.
7. Жавгуряну, В.Н.; Годеленко, П. Соотношение восстановленной и невостановленой микротвердости хромовых покрытий. Международная НТК "Машиностроение и техносфера XXI века", Севастополь, 2005.
8. Жавгуряну, В.Н. Исследование работы деформации износостойких гальванических покрытий при микровдавливании. Международная НТК "Новые процессы и их модели в ресурсо и энергосберегающих технологий", Одесса, 2003, с. 7-8.

Prezentat la redacţie la 4.12.2013

CZU 620.9 (075.8)

FEATURES OF ELASTOPLASTIC DEFORMATIONS OF COMPOSITE IRON-NICKEL COATINGS AND THEIR IMPACT ON THE INTENSITY OF WEAR

Javgureanu V.*, Gordelenco P.
Universitatea Tehnică a Moldovei, bd. Ştefan cel Mare, 168, MD-2004, Chişinău, Republica Moldova
*e-mail: v_javgureanu@yahoo.com

Lucrare prezintă caracteristicile deformaţiilor elastoplastice şi a ruperii fragile a acoperirilor compozite de fier-nichel obţinute prin depunerea electrolitică. Caracteristicile fizico-mecanice (H_h; H_d; A_e; A_p; A; P; H_h/E; H_d/E) pot fi utilizate pentru a perfecţiona descrierea vitezei de uzurăa acoperirilor de fier-nichel.

Cuvinte-cheie: acoperiri de fier-nichel, compozit, viteză de uzură, proprietăţile fizico-mecanice, deformaţiile elastoplastice.

The paper presents some features of elastoplastic deformation and brittle fracture of iron-nickel composite coatings obtained at electrolyte deposition. Physico-mechanical characteristics (H_h; H_d; A_e; A_p; A; P; H_h/E; H_d/E) can be used to improve the description of wear rate of iron-nickel coatings.

Keywords: iron-nichel coatings, composite, wear rate, physico-mechanical properties, elastoplastic deformation.

1. INTRODUCTION

Electrolytic wear-resistant coatings are widely used for hardening and restoration parts in the industry in order to increase their longevity. Electrodeposition conditions have a significant impact on the physical and mechanical properties of wear-resistant plating. Knowledge of physical and mechanical characteristics of wear-resistant plating needed to make informed choices technological conditions of deposition, depending on the operating conditions of the recovered parts of machines, as well as for important structural calculations [1-3].

2. GENERAL INFORMATION

Actual problems of study of physical and mechanical properties of materials in the surface and the surface layers due to the fact that the deformations associated with contact with modern methods of treatment and hardened metal compounds. Test kinetic hardness and microhardness opens up new possibilities for the determination of physical and mechanical properties and fracture toughness of electrolytic plating coating [1-3].

An important parameter in the study of physical and mechanical characteristics of wear-resistant plating is their fragility. This property plating is undesirable since the craze fragility affects such important characteristic as wear resistance [2]. The importance of identifying the characteristics of elastic-plastic (**he**, **hp**, **h**) required for robot deformation (**Ae**, **Ap**, **A**), unrestored and dynamic hardness (**Hh**, **Hd**) modulus (**E**), the critical load indentation diamond spherical indenter with a start brittle fracture ($\mathbf{P_{CR}}$), the ratio of non-reduced and dynamic hardness to elastic modulus (**Hh/E, Hd/E**), yield strength ($\boldsymbol{\sigma_T}$), the true tensile strength ($\mathbf{S_B}$), tensile strength ($\boldsymbol{\sigma_b}$), yield strength ($\boldsymbol{\sigma_{0,2}}$) toughness ($a_H$), the degree of deformation of the material in the contact zone ($\boldsymbol{\psi}$) is invaluable.

The paper presents some features of elastoplastic deformation and brittle fracture of iron-nickel composite coatings obtained from electrolyte 4 [2, p. 59]. The samples used rollers with diameter 30 mm, thickness of the coating 0.5 mm and a length of 100 mm, which were processed under optimal grinding. Physico-mechanical characteristics were determined at the facility for the study of the hardness of materials in macrovolume equipped with an inductive sensor and a differential amplifier allows you to record chart indentation diamond spherical indenter and indentation recovery after removal of the load [2].

Dynamic hardness (**Hd**) was determined as the ratio of the total work expended by elastoplastic deformation of (**A**) to the volume of deformable material (**V**) under load, in all investigated iron-nickel composite coating.

3. DISCUSSION OF EXPERIMENTAL RESEARCH

Studies have shown that the investigated physical and mechanical properties of iron-nickel composite coatings vary with the electrolysis conditions (tables 1 and 2).

Table 1

Physico-mechanical properties of Fe-Ni composite coatings

Electrolysis conditions		***Work expended on the deformation of coatings***			H_h N/mm^2 (h=2μm)	H_d N/mm^2	P, N	P_{cr}, N	E, $\times10^{-4}$, N/mm^2	H_h/E	H_d/E
Dк, $\times10^{-4}$ kA/m^2	T, ˚C	A_e N·mm	A_p N·mm	A N·mm							
5	40	0.0172	0.0132	0.0304	3630	2422	45.6	350	21.0	0.0173	0.0115
10	40	0.0177	0.0135	0.0312	3670	2449	46.1	335	20.5	0.0179	0.0119
20	40	0.0186	0.0132	0.0318	3800	2534	47.7	320	19.8	0.0192	0.0128
30	40	0.0202	0.0132	0.0334	3980	2686	50.0	300	19.5	0.0204	0.0136
40	40	0.0214	0.0132	0.0346	4120	2746	51.7	275	19.3	0.0213	0.0142
50	40	0.0235	0.0138	0.0373	4470	2980	56.1	260	18.8	0.0238	0.0159
60	40	0.0202	0.0121	0.0323	4020	2683	50.5	245	18.0	0.0223	0.0149
80	40	0.0188	0.009	0.0278	3320	2215	41.7	215	17.5	0.0190	0.0127

With increasing current density (**Dk**) of 5×10^{-4} to 80×10^{-4} kA/m^2 electrolysis at a constant temperature (40 ^{o}C), the critical load (**Pcr**) and the iron-nickel coatings modulus (**E**) is reduced accordingly from 350 to 215 (**H**) and from 21×10^{-4} to 17.5×10^{-4} (N/mm^2). Work expended in elastic (**Ae**), plastic (**Ap**), unrestored hardness (**Hd**), dynamic hardness (**Hd**), the indentation load on the diamond spherical indenter (**P**) ratio **Hh/E** and **Hd/E** have extreme values with the change of the current density (**Dk**) from 5×10^{-4} kA/m^2 80×10^{-4} kA/m^2 to electrolysis at a constant temperature (40 °C). Physico-mechanical properties of iron-nickel coatings (table 1 and 2) determined for one indentation depth (h=2μm) by a known method [2].

Studies have shown that with increasing current density of 5×10^{-4} to 50×10^{-4} kA/m^2 electrolyte at a constant temperature (40 °C) the work expended in elastic deformation coverage increased from 17.2×10^{-3} to 23.5×10^{-3} (N·mm), the work expended in plastic deformation, coatings increased from 13.2×10^{-3} to 13.8×10^{-3} (N·mm), the total work spent on elastoplastic deformation of the coating increased from 30.4×10^{-3} to 37.3×10^{-3} (N·mm). With further increase of the current density of 50×10^{-4} to 80×10^{-4} kA/m^2, electrolysis at a constant temperature (40 °C) work spent on elastic deformation of coatings decreased from 23.5×10^{-3} to 18.8×10^{-3} (N·mm) total work spent on plastic deformation decreased from 13.8×10^{-3} to 9.0×10^{-3} (N·mm), the total work spent on elastoplastic deformation of coatings decreased from 37.3×10^{-3} to 27.8×10^{-3} (N·mm). From the results of research can be seen that the work expended in elastic (**Ae**), plastic (**Ap**) and elastic-plastic (**A**) deformation of iron-nickel coatings at a constant temperature electrolysis are extreme.

Character changes unreduced hardness (**Hh**), dynamic hardness (**Hd**) and extrusion load the diamond spherical indenter at a depth of 2 μm with increasing current density of 5×10^{-4} to 80×10^{-4} (kA/m^2), at a constant temperature electrolysis (40 °C) has an extreme character.

With increasing current density of 5×10^{-4} to 50×10^{-4} (kA/m^2) unrestored coating hardness (**Hh**) increased from 3630 to 4470 (N/mm^2), dynamic coating hardness **Hd** increased from 2422 to 2980 (N/mm^2) and the indentation load on the diamond spherical indenter (**P**) increased from 45.6 to 56.1 (N). With further increase in current density (**DK**) from 50×10^{-4} to 80×10^{-4} (kA/m^2) at constant temperature electrolysis (40 °C) hardness unrestored (**Hh**) decreased from 4470 to 3320 (N/mm^2) dynamic coating hardness decreased from 2980 to 2215 (N/mm^2) and the

indentation load on the diamond spherical indenter decreased from 56.1 to 41.7 (N) (table 1).

With increasing temperature electrolysis (T, Table 2) at a constant current density (D_K=50×10^{-4} kA/m^2) from 20 to 60 ^{o}C, the critical load indentation on diamond spherical indenter characterizes the beginning of brittle fracture of iron-nickel coatings and the elastic modulus of the coating increases, respectively, from 205 to 315 (N) and from 17.1×10^{-4} to 20.5×10^{-4} (N/mm^2).

Table 2

Physico-mechanical properties of Fe-Ni composite coatings

Electrolysis conditions		***Work expended on the deformation of coatings***			Hh N/mm^2 (h=2μm)	Hd, N/mm^2	P, N	Pcr, N	E, ×10^{-4} N/mm^2	Hh/E	Hd/E
Dк, ×10^{-4} kA/m^2	T, ˚C	Ae, N·mm	Ap, N·mm	A, N·mm							
50	20	0,0211	0,0067	0,0278	3320	2215	41,7	205	17,1	0,0194	0,013
50	40	0,0235	0,0148	0,0383	4470	2980	56,1	260	18,8	0,0238	0,0159
50	60	0,0156	0,0138	0,0294	3630	2422	45,6	315	20,5	0,0177	0,0118

Nature of the change work expended in elastic (**Ae**), plastic (**Ap**) and elastic-plastic deformation (**A**) of iron-nickel coatings with temperature electrolysis from 20 to 60°C at a constant current density (Dk=50×10^{-4} kA/m^2) also has an extreme character. With increasing temperature, the cell from 20 to 40 °C at a constant current density (Dk=50×10^{-4} kA/m^2), the work expended in elastic (**Ae**), plastic (**Ap**) and elastic-plastic deformed (**A**) increased respectively from 21.1×10^{-3} to 23.5 ×10^{-3} (N·mm) from 6.7×10^{-3} to 14.8×10^{-3} (N·mm), and from 27.8×10^{-3} to 38.3×10^{-3} (N·mm). With further increase of the temperature (**T**) of the cell from 40 to 60 °C at a constant current density (Dk=50×10^{-4} kA/m^2) work spent on elastic (**Ae**), plastic (**Ap**) and elastic-plastic deformation (**A**) iron-nickel coatings decreased correspondingly from 23.5×10^{-3} to 15.6×10^{-3} (N·mm) of 14.8×10^{-3} to 13.8×10^{-3} (N·mm), and from 38.3×10^{-3} to 29.4×10^{-3} (N·mm).

Character of change of hardness unreduced (**Hh**), a dynamic hardness (**Hd**), and the load - spherical indentation diamond indenter at a depth of 2 microns from the electrolysis temperature increases from 20 to 60 °C at a constant current density (Dk=50×10^{-4} kA/m^2) have also extreme. With increasing temperature electrolysis (**T**) from 20 to 40 °C at a constant current density (Dk=50×10^{-4} kA/m^2) unrestored hardness (Hh) has increased from 3320 to 4470 (N/mm^2), dynamic hardness (**Hd**) increased from 2215 to 2980 (N/mm^2), and the load - indentation diamond spherical indenter (**P**) increased from 41.7 to 56.1 (N). With further increase of the temperature of the cell from 40 to 60 °C at a constant current density (Dk=50×10^{-4} kA/m^2) not restored hardness (Hh) decreased from 4470 to 2422 (N/mm^2), dynamic hardness (**Hd**) decreased from 2980 to 2422 (N/mm^2), and the load - indentation diamond spherical indenter (**P**) decreased from 56.1 to 46.5 (N).

Much attention in the study of physical and mechanical properties of wear-resistant plating on defining their tendency to brittle fracture. The fragility of the coating is significantly affected by the conditions of their electrodepositing [2].

Increase in current density (**Dk**) and the electrolysis temperature (**T**) coatings tendency to brittle fracture increases. Composition of the electrolyte, which is obtained from wear-resistant coatings, can have a different impact on the considered properties of the coatings [2].

It was proved that the method of measuring the hardness of the coatings at different loads (up to **Pcr**) unrestored hardness (**Hh**) is constant. With further increase in load (>**Pcr**) is the value rises sharply, indicating a deviation from the mechanical similarity. On the regularities of a significant influence of electrolysis conditions coatings [2].

With increasing current density and decreasing temperature electrolysis violation original pattern passes with less pressure on the diamond spherical indenter [2-8].

In studying the characteristics of elastic and plastic deformation of iron-nickel coatings obtained after processing the indentation diagrams showed that responsible for the results is the change in the character of elastic deformation depending on the loading condition.

Regardless of the subject to the iron-nickel coatings with increasing load on the diamond - spherical indenter elastic deformation component coatings first increase dramatically (up to **Pcr**) and then rises slightly (after **Pcr**).

This proves that the main reason causing the violation of the law of the mechanical similarity due to the onset of brittle fracture of iron-nickel coatings [1].

Comparing the value of critical load indentation (**Pcr**) for spherical diamond indenter with their values determined by observation of the formation of ring cracks around the indentation, it can be argued that the beginning of the destruction of the coatings can be determined much more accurately by measuring the indentation depth (**h**) and diamond spherical indenter critical load (**Pcr**), as to the formation of an annular crack growth is possible source and the formation of new cracks are difficult to watch for. Critical stress ($\mathbf{Hh_{cr}}$) can be taken as a criterion for evaluating the tendency to brittle fracture coatings.

Studying the effect of current density (**Dk**) and the electrolysis temperature (**T**) on the tendency of iron nickel coatings to brittle fracture showed that with increasing current density of 5×10^{-4} to 80×10^{-4} (kA/m^2) at a constant temperature electrolysis (40 °C) critical load indentation on diamond spherical indenter is reduced from 350 to 215 (H), indicating an increase in the propensity of iron-nickel coating to brittle fracture. With increasing temperature, the cell from 20 to 60 °C at a constant current density (Dk=50×10^{-4} kA/m^2), the critical load indentation on diamond spherical indenter is increased from 205 to 315 (N), indicating a decline in the propensity to brittle iron-nickel coatings destruction.

One of the problems of engineering is predicting wear resistance of materials. In that sense, the hardness test method applies to micromechanical testing, allowing the most reasonable approach to these material characteristics.

We obtained dimensional parameters **Hh**, **Hd**, **P**, **Pcr**, and the dimensionless **Hh/E** and **Hd/E** have a good correlation with the wear rate wear resistance of iron-nickel composite coatings. Ratio **Hh/E** and **Hd/E** into account the elastoplastic properties of iron-nickel coatings accurately describe the process of wear.

Thus parameters **Hh**, **Hd**, **Hh/E** and **Hd/E** can be used to further clarify the description of the wear rate on these parameters and is based on the concept of additive contributions of these structural indicators (1.3-8).

The results showed that the ratio **Hh/E** and **Hd/E** elastoplastic characteristics into account, iron-nickel coatings have extreme value, as previously discussed parameters (**Ae**, **Ap**, **A**, **Hh**, **Hd**, **P**) with a change in the electrolysis conditions (**Dk**, **T**) for obtaining optimal properties of iron-nickel coatings in terms of their durability.

With increasing current density (**Dk**) of 5×10^{-4} to 50×10^{-4} (kA/m^2) at a constant temperature of electrolysis (40 °C) the ratio **Hh/Hd** and E/E (table 1), respectively, increases from 17.3×10^{-3} to 23.8×10^{-3} and 11.5×10^{-3} to 15.9×10^{-3}. With a further increase in current density (**Dk**) from 50×10^{-4} to 80×10^{-4} (kA/m^2) at a constant temperature of electrolysis (40 °C), the ratio **Hh/Hd** and **E/E** accordingly reduced from 23.8×10^{-3} to 19×10^{-3} and from 15.9×10^{-3} to 12.7×10^{-3}.

With increasing temperature electrolysis (**T**) from 20 to 40 °C at a constant current density (Dk=50×10^{-4} kA/m^2) ratio **Hh/E** and **Hd/E** increases from 19.4×10^{-3} to 23.8×10^{-3} and from 13×10^{-3} to 15.9×10^{-3}. With further increase of the temperature of the cell from 40 to 60 °C at a constant current density (Dk=50×10^{-4} kA/m^2) ratio **Hh/E** and Hd/E reduced accordingly from 23.8×10^{-3} to 17.7×10^{-3} and from 15.9×10^{-3} to 11.8×10^{-3}.

To evaluate the ability to predict the wear resistance of friction pairs as measured by thermal resistance of the boundary layer lubrication, anti-friction and physics - the mechanical properties of studies have been conducted to determine the wear of iron - nickel coatings rubbing against doped feed lubrication **M12B**. To assess the effect of physical - mechanical properties (**Ae**, **Ap**; **A**, **Hh**; **Hd**; **P**; **Pcr**; **Hh/E**; **Hd/E**) on the wear resistance of iron - nickel coatings studied the effect of current density (**Dk**) and the electrolysis temperature (**T**) on the wear resistance of the alloy iron - nickel (table 3 and 4) rubbing against alloyed iron feed lubrication **M12B**. Burnishing sampling began spending 150 N/cm^2 under load, which is then gradually increased to work. Closing break-in was fixed in magnitude of the frictional moment in the vicinity of the zone temperature friction and wear control by measuring the amount of samples. Duration wear chosen in light of the values of wear.

Microprobe analysis of iron - nickel plating conducted microanalyzer **MS-46** showed that increasing the current density of the nickel content in the coating decreases and increases with increasing temperature distribution besides nickel coating thickness is uniform, except for the exit area mode.

Table 3

Physico-mechanical properties and the wear rate of iron-nickel coatings rubbing against alloyed iron in the presence of oil M12B

Electrolysis conditions		***Work expended on the deformation of coatings***			Hh, N/mm^2 (h=2μm)	Hd, N/mm^2	P, N	Pcr, N	Hh/E	Hd/E	I, mg/hour
Dк, $\times10^{-4}$ kA/m^2	T, ˚C	Ae, N·mm	Ap, N·mm	A, N·mm							
5	40	0.0172	0.0132	0.0304	3630	2422	45.6	350	0.0173	0.0115	-
10	40	0.0177	0.0135	0.0312	3670	2449	46.1	335	0.0179	0.0119	4.8
20	40	0.0186	0.0132	0.0318	3800	2534	47.7	320	0.0192	0.0128	3.9
30	40	0.0202	0.0132	0.0334	2980	2556	50.0	300	0.0204	0.0136	2.6
40	40	0.0214	0.0132	0.0346	4120	2746	51.7	275	0.0213	0.0142	2.2
50	40	0.0235	0.0138	0.0373	4470	2980	56.1	260	0.0238	0.0159	1.8
60	40	0.0202	0.0121	0.323	4020	2683	50.5	245	0.0293	0.0149	2.6
80	40	0.0188	0.0090	0.0278	3320	2215	41.7	215	0.0190	0.0127	3.9

Table 4

Physico-mechanical properties and the wear rate of iron-nickel coatings rubbing against alloyed iron in the presence of oil M12B

Electrolysis conditions		***Work expended on the deformation of coatings***			Hh, N/mm^2 (h=2μm)	Hd, N/mm^2	P, N	Pcr, N	Hh/E	Hd/E	I, mg/hour
Dк, $\times10^{-4}$ kA/m^2	T, ˚C	Ae, N·mm	Ap, N·mm	A, N·mm							
50	20	0.0211	0.0067	0.0278	3320	2215	41.7	205	0.0194	0.0130	2.42
50	40	0.0235	0.0148	0.0373	4470	2980	56.1	260	0.0238	0.0759	1.80
50	60	0.0156	0.0138	0.0294	3630	2422	45.6	315	0.0177	0.0118	2.21

To determine the effect of current density (**Dk**) and the electrolysis temperature (**T**) on the wear rate (tables 3 and 4) iron alloy coatings - nickel and its relationship with the physical - mechanical properties macrovolume (**Ae**, **Ap; A, Hh; Hd; P; Pcr; Hh/E; Hd/E**) specific tests. Precipitation of iron nickel alloy were obtained at a current density of 10×10^{-4}, 20×10^{-4}, 30×10^{-4}; 40×10^{-4}, 50×10^{-4}, 60×10^{-4} and 80×10^{-4} kA/m^2, wherein the electrolysis temperature was 40 °C, P_H=0.8÷1.0, which are worn in conjunction with iron - doped (table 3).

Other iron- nickel alloy precipitation were obtained at a current density of 50×10^{-4} kA/m^2, wherein the electrolysis temperature was varied 20, 40 and 60 °C at P_H=0.8÷1.0 (table 4) who also wore conjugation doped with iron.

Studies have shown that increasing the current density (**Dk**) from 10×10^{-4} to 50×10^{-4} (kA/m^2) at the electrolysis temperature 40 °C, P_H=0.8÷1.0 wear rate decreased from 4.8 to 1.8 (mg/hour) and then increased to 1.8 to 3.9 (mg/hour) (table 3), with increasing the current density (**Dk**) from 50×10^{-4} to 80×10^{-4} (kA/m^2).

With increasing temperature, the electrolysis of from 20 to 40 °C at a current density of 50×10^{-4} kA/m^2, P_H=0.8÷1.0 wear rate decreased from 2.4 to 1.8 (mg/hour). With further increase of the electrolysis temperature of 40 to 60 °C at a current density of 50×10^{-4} kA/m^2, P_H=0.8÷1.0 wear rate increased from 2.21 to 1.8 (mg/hour) (table 4).

The data patterns are in good agreement with the effect of the current density (**Dk**) and the electrolysis temperature (**T**) on the physical - mechanical characteristics of the iron-nickel coatings, temperature stability (**Tcr**) and wear rate of the coatings (table 3 and 4).

With increasing physico-mechanical properties of iron-nickel coatings (**Ae**, **Ap**; **A**, **Hh**; **Hd**; **P**; **Pcr**; **Hh**/**E**; **Hd**/**E**) (table 1 and 2) increased durability and improved anti-friction properties of an alloy of nickel and iron alloy cast iron.

Thus maximal values of physical - mechanical characteristics (**Ae**, **Ap**; **A**, **Hh**; **Hd**; **P**; **Pcr**; **Hh**/**E**; **Hd**/**E**) iron nickel coatings can make a selection of coatings obtained under different conditions of electrolysis in terms of their maximum durability. This will significantly reduce the time of the experiments, increasing the volume research that will significantly expand the scope of effectiveness studies iron nickel coatings industry.

4. CONCLUSION

It was established experimentally that the unreduced hardness (**Hh**), dynamic hardness (**Hd**), the work expended in elastic (**Ae**), plastic (**Ap**) elastic-plastic (**A**) deformation, the load on a spherical diamond indenter (**P** for **h**=2μm) ratio **Hh**/**E** and **Hd**/**E** is experimental conditions change electrolysis (**Dk**, **T**) for the study of iron-nickel coatings.

Experimental value unreduced hardness (**Hh**) dynamic hardness (**Hd**), the work expended in elastic (**Ae**), plastic (**Ap**), elastoplastic deformation (**A**) load on a spherical diamond indenter (**P**), the ratio **Hh**/**E** and **Hd**/**E** coincides with our earlier recommendations for iron-nickel coatings in terms of ensuring their optimum durability.

Experimentally established the beginning of brittle fracture of iron-nickel coatings (**Pcr**, **Hh_{cr}**) with the changed conditions of electrolysis (**Dk**, **T**), the critical load (**Pcr**) indentation on diamond spherical indenter and the critical stress (**Hh_{cr}**), which can be taken as a criterion for evaluating the tendency of coatings to brittle fracture.

The method of measuring the hardness in macrovolume allows most reasonably and accurately determine the physical and mechanical characteristics (**H_h**; **H_d**; **A_e**; **A_p**; **A**; **P**; **H_h**/**E**; **H_d**/**E**) iron-nickel coatings.

Physico-mechanical characteristics (**H_h**; **H_d**; **A_e**; **A_p**; **A**; **P**; **H_h**/**E**; **H_d**/**E**) iron-nickel coatings have good correlation with the intensity of wear of these coatings.

Physico-mechanical characteristics (**H_h**; **H_d**; **A_e**; **A_p**; **A**; **P**; **H_h**/**E**; **H_d**/**E**) can be used to refine the description of the wear rate of iron-nickel coatings.

BIBLIOGRAPHY

1. Булычев, С. И.; Алехин В. Н. Испытание материалов непрерывным вдавливанием индентора. Москва, Машиностроение, 1990, 224с.
2. Гологан, В. Ф.; Аждер, В. В.; Жавгуряну, В. Н. Повышение долговечности деталей машин износостойкими покрытиями. Кишинев, Изд-во Штиинца, 1979, 112 с.

3. Javgureanu, V.; Ajder, V.; Ceban, V.; Pavlova. The correlation of restored and unrestored microhardness of. Wear-proof iron plating. Conferinţă Ştiinţifică Internaţională TMCR. Chişinău, 2003, p. 412-415.
4. Javgureanu, V.; Gordelenco, P.; Elita, M. The work of deforming wear -proof iron-nikel plating in microsquelging. The Annals of University "Dunărea de Jos" of Galaţi, Fascicle VIII, 2004, Tribology, Romania, pp.65-68.
5. Javgureanu, V.; Gordelenco, P.; Elita, M. Relationship of the restored and unrestored microharedbess of the cromium coating. The Annals of University "Dunărea de Jos" of Galaţi, Fascicle VIII, 2004 Tribology, Romania, pp.48-51.
6. Javgureanu, V.; Gordelenco, P.; Elita, M. Le rapport de la microdurete restauree et non restauree des convertures de crome. Conferinţă Ştiinţifică Internaţională TMCR, Chişinău, 2005, pp. 166-169.
7. Жавгуряну, В.Н.; Годеленко, П. Соотношение восстановленной и невостановленой микротвердости хромовых покрытий. Международная НТК "Машиностроение и техносфера XXI века", Севастополь, 2005.
8. Жавгуряну, В.Н. Исследование работы деформации износостойких гальванических покрытий при микровдавливании. Международная НТК "Новые процессы и их модели в ресурсо и энергосберегающих технологий", Одесса, 2003, с.7-8.

Prezentat la redacţie la 4.12.2013

CZU 621.0.484

RESEARCH ON ELECTRO-SPARK ALLOYING REGULARITIES AT ADDITIONAL ACTION ON THE PROCESS BY ELECTRIC CURRENT

Pereteatcu P.*, Cracan C.
Alecu Russo Balti State University, Pushkin Str. 38, MD-3100, Balti, Republic of Moldova
*e-mail: pereteatcupavel@yahoo.com

Regularităţile alierii prin scîntei electrice cu acţiunea suplimentară asupra procesului a curentului electric se studiază în acest articol. Experimental s-a stabilit că, sub acţiunea suplimentară a curentului electric care trece prin piesa de lucru-catod, viteza de formare a straturilor de depunere creşte de cca. 2-4 ori şi sporeşte calitatea suprafeţei prelucrate.

Cuvinte-cheie: aliere prin scîntei electrice, curent electric, adaosul de masă catodică, calitatea suprafeţei.

Regularities of electro-spark alloying at additional action on the process by electric current are studied in this paper. It was experimentally established that, under the supplementary action of the electric current passing through the workpiece-cathode, the speed of deposition layer formation increases by about 2-4 times and the quality of the machined surface enhances.

Keywords: electro-spark alloying, electric current, cathode mass growth, surface quality.

It is known that one of the technologies used in structures and physico-mechanical properties modifying of the alloys on their surface is electro-spark alloying (ESA) [1].

To realize the ESA processing it is necessary firstly the electric erosion prcocesses and directional mass transfer of electrodes material to take place [1-3]. But these conditions are not sufficient for the transferred material to bind strongly with cathode-matrix. In general, the amount of material removed from the anode at the ASE process is directly proportional to the spark discharge energy ($\gamma \equiv W$), and this dependence is maintained strictly for the specific values of discharge power ($W \leq 1$ T) and the process duration.

At the same time, it is necessary to emphasize that a number of factors, such as the nature of the electrode material and the parameters of the process (electrode geometry, shape of their movement, etc.) influences on the character of material transfer from the anode to the cathode.

The dynamics of surface layers formation on the cathode at the ASE process is characterized by the fact that the material transfer intensity from the anode on the cathode, which is maximal in the first moments of the process performing, decreases with time. Finally, for certain values of discharge energy, the inversion of previously deposited material transfer, ie its erosion, takes place.

Thus, the concurrence between formation and deterioration processes of deposited layers with predominance of the last, with increasing processing time, leads to limiting formed layer thickness [3-5]. To solve this difficult problem, as noted in several works [2, 3] - ESA can be realized in vacuum or inert medium (argon, helium) or relaxation annealing of the cathode can be performed etc. But no one of these methods gives good results and allows the definitive solution of this problem. It is obvious the need to find another way, which implies the possibility of directing the transfer and electrode material interaction processes without changing (increasing) the parameters of the discharge energy, by the action of external factors. These factors, as mentioned in [6] can be electric current, whose value can be varied (increased or decreased) in the higher limits. Preliminary results showed that the direct action of not high value electric current of about 0.5-2.5 A, (current passes both through anode and cathode) leads to substantially increase the material transfer processes and physico-chemical transformations in the cathode layers.

In this context, we studied the possibility to intensify the ESA process by the pass of the electric current through electrodes volume.

For this purpose, anode and cathode (or both simultaneously) when alloying were introduced into the circuit of continuous or pulsating current which value had been adjusted in large limits depending on the processing time. The results were compared with data obtained in the absence of current, i.e. with those obtained by traditional processing.

The electrodes with diameter of 1.5-3.0 mm and length of 40 mm, made of crome, nickel, silver, alloys „VJL-2" and „VJL-14", hard alloys „VK8" and „T15K6" were used as anodes, and the samples made of steel „St-3", „St-45", copper M1, titan BT1 were used as cathodes.

The continuous current varied in such a way ensuring the current density from 0.5 to 5 A/mm^2 through the anode section. The pulsating current with electrical impulses shape, duration of 150-200 μs and amplitude of 200-600 A also passed through the anode. These parameters of electric current were chosen from the condition that passing through the anode its substantial erosion increase to take place during the spark discharge, and therefore it will accelerate the formation of coating layer on the cathode.

Experimental results have shown that for an insignificant amount of current density of 0.5...1.0 A/mm^2, which passes through the anode, the increase of its erosion takes place.

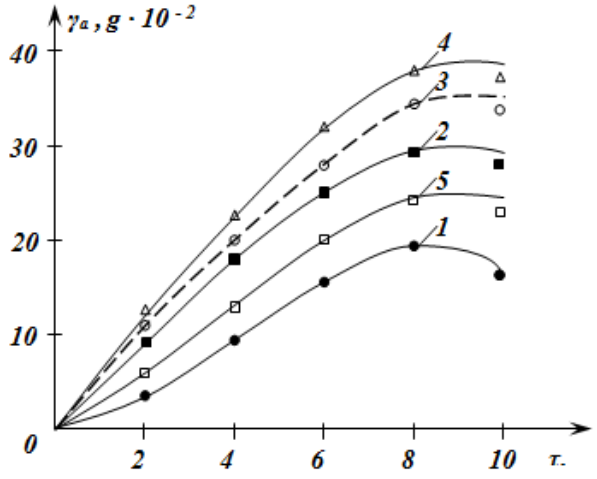

Fig. 1. Time dependence of anode erosion on the current density passing through it (Installation EFI – 10M, regime no. 3): 1 – I = 0 A/mm^2; 2 – I = 0,5 A/mm^2; 3 – I = 1,0 A/mm^2; 4 – I = 2,4 A/mm^2; 5 – I = 4,0 A/mm^2

For example, for specific work-time equal to 4 min/cm^2, the amount of material removed from the anode, through which the current with density of 2.4 A/mm^2 passes, is 2 times higher than by usual ESA at the same regime. However, for the current passing through the anode with a density of 4.0 A/mm^2 there is a decrease in the amount of material removed from the anode (Fig. 1, curve 5).

An analog picture is observed when passing through the anode a pulsating current of 200-600 A with duration of 200 μs. In this case there is also a critical current value, above which the erosion effect slows down. This corresponds to the current value of 250 A.

Determining the transfer coefficient of the material, it has been found that its amount increases not significantly comparatively with the same by traditional alloying, i.e. substantially increase of anode erosion by current passing through it has a very small influence on its adhesion with the cathode material. This shows that the current passing through the anode during ESA predominantly influences the erosion of the anode and insignificant influences processes arising in the superficial layers of the cathode and, therefore, it is obvious that such a processing scheme is only a partial solution of ESA process intensification and its enhance in practical use is unreasonable.

Besides this, the manufacture of anodes need special resources which are small due to the small size of the work sector, which makes this process to be non-technological and, therefore, another ESA scheme was used further, when the electric current passed through the cathode.

Concretely, while using cathodes made of iron and copper the highest transfer is observed when the current with density of 0.5...3A/mm^2 passes through the cathode. Further increase of the current leads to the reduction in time of the cathode mass (Fig. 2), and for the value of current density of 4 A/mm^2 the dynamic of mass increase is analogous to that observed in the case of traditional alloying.

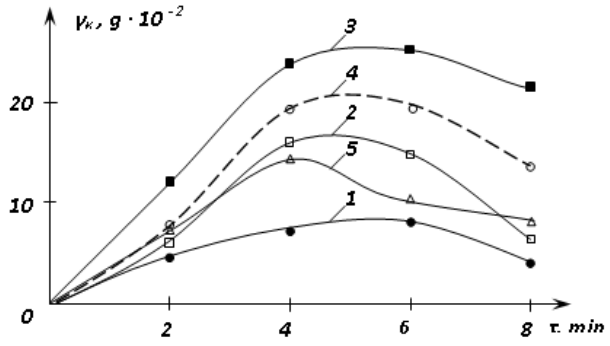

Fig. 2. Dependence of cathode mass growth in time on the current density passing through it:
1 – I = 0 A/mm^2; 2 – I = 2,0 A/mm^2; 3 – I = 3,0 A/mm^2; 4 – I = 4,0 A/mm^2; 5 – I = 5,0 A/mm^2

Similar results were obtained when pulsating current passed through the cathode (Fig. 3).

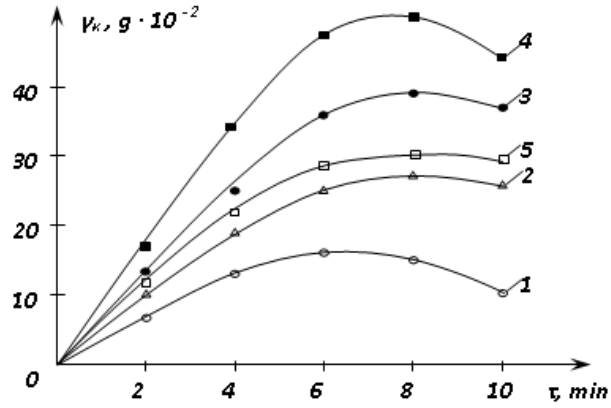

Fig.3. Dependence of cathode mass growth in time on the value of pulsating current passing through it (Installation EFI – 10M, regime no. 3; anode – Ag, cathode – Cu.; current impulse duration – 200 μs).
1 – $I_и$ = 0 A ; 2 – $I_и$ = 100 A ; 3 – $I_и$ = 200 A ; 4 – $I_и$ = 400 A ; 5 – $I_и$ = 600 A

Analysis of these data showed that the increase in mass of the cathode when the electric current passes through it takes place not because of more intensive erosion of the anode, but as a result of more favorable conditions, which are created on the cathode during the passing of current through it, where most eroded mass coats and interacts with the cathode (substrate). One of the probable factors that influence the intensification of eroded mass transfer on the cathode can be improvement of wetting and stretching of the anode liquid material transferred on the cathode at the spark discharge. A good spread of the liquid phase on the cathode surface probably contributed to "cure" the defects (pores, micro-cracks) which ultimately reduce the action of factors which limit the increase of deposited layer.

By examining the curves in Fig. 4 we can see that the peak is situated far above the axis and is shifted to the right that talks us about more slow accumulation of stretch residual tensions in layers leading to deterioration of the formed surface layer.

At the alloying with anodes made of fragile materials the effect of improvement in transfer is highlighted less, which can probably be explained by the formation of small quantities of eroded liquid mass.

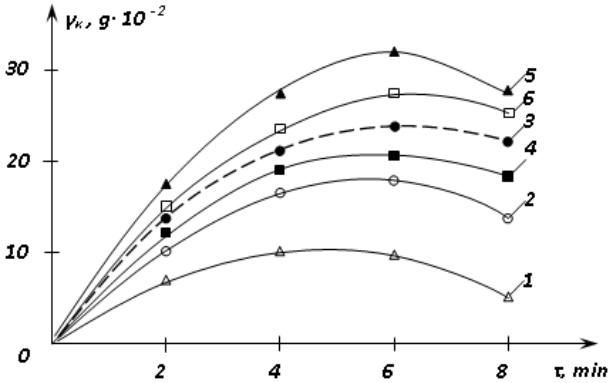

Fig. 4. Time dependence of cathode mass growth at ESA and the pass of the current with different density (cathode material – steel „St-3”, installation EFI – 10M, regime no. 3):
1 – J = 0 A/mm^2; 2 – J = 4 A/mm^2; 3 – J = 1,2 A/mm^2; 4 – J = 1,7 A/mm^2; 5 – J = 2,4 A/mm^2; 6 – J = 3 A/mm^2

For example, at the alloying with anodes made of alloy “ВК20” (with 20% cobalt) the mass transfer is of 1,2-2 times greater than it is at the processing under the same conditions (equal discharge energy and current) with anodes made of “ВК8” (containing 8% cobalt) (Fig. 5).

At the same time, it is necessary to mention that there is a critical value of the current passing through the cathode, then there is a decrease in the amount of anode material deposited on the cathode surface, which can also be explained by increasing the tensile forces till such a value at which the break of the formed pellicle from the metal drop transferred on the cathode takes place.

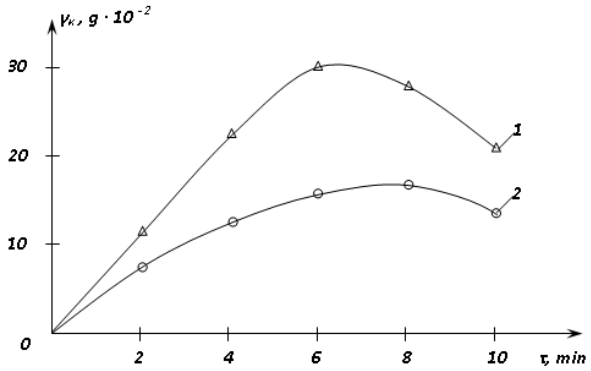

Fig. 5. Variation of the cathode mass growth change in time at alloying with anodes made of different materials but at the same current density passing through the cathode
(Installation EFI – 54A, regime no. 1, I = 2,6 A/mm^2):
1 – BK20; 2 – BK8

CONCLUSION

Therefore, the direct action of external forces on the electrodes, in particular, the current passing through the cathode leads to a 2-4 times increase in the speed of the surface layer formation on the cathode, to improve the quality of these layers (roughness reducing, uniformity increase, etc.) and to widen the set of materials, on which can be deposited coatings with additional influence of the electric current passing through the cathode that in conditions of usual ESA is difficult to obtain.

BIBLIOGRAPHY

1. Лазаренко Н.И. Измененме исходных свойств поверхности катода под действием искровых электрических импульсов протекающих в газовой среде. В кн. Электроискровая обработка металлов, вып. 1, М. Изд-во АН СССР, 1957, с. 70-94.
2. Лазаренко Н.И. Технологический процесс изменения исходных свойств металлических поверхностей электрическими импульсами. В кн. Электроискровая обработка металлов, вып.2, М., Изд-во АН СССР, 1960, с. 26-66.
3. Гитлевич А.Е., Михайлов В.В., Парканский Н.Я., Ревуцкий В.М. Электроискровое легирование металлических поверхностей. Под ред. акад. АН МССР Ю.Н.Петрова, Кишинев, Штиинца, 1985. 195 с.
4. Палатник Л.С. Рентгенографические исследования превращений в поверхностном слое металлов, подвергшихся действию электрических разраядов. Изд. АН СССР сер. Физ., 1951, 15 №1, с. 80-86.
5. Палатник Л.С. Фазовые превращения при электроискровой обработке металлов и опыт установления критерия наблюдаемых взаимодействий. Д. АН СССР, 1953, 89, №3, с. 455.
6. Bibly M.T., Nutchinson L.T., Toudis W.V. Direct electric field electrotransport of carbon and nitrogen in iron and iron alloys. Can. T. Phys, 1966, 44, p. 2375-2386.

Prezentat la redacţie la 1 august 2013

CZU 533.9.07

ELECTROD DESTINAT OBŢINERII PLASMEI ÎN IMPULS CU FUNCŢIE DUBLĂ

Hîrbu A.
Universitatea de Stat „Alecu Russo” din Bălţi, str. Puşkin 38, MD-3100, Bălţi, Republica Moldova
e-mail: arefahirbu@yahoo.com

Lucrarea rezolvă problema elaborării unui dispozitiv – electrod-multicanal care asigură obţinerea plasmei în impuls cu autoionizarea mediului activ (fără dispozitive auxiliare) şi scporirea duratei de funcţionare a lui (în lipsa distrugerii canalelor de descărcare). Electrodul elaborat îndeplineşte funcţie dublă: serveşte iniţial în calitate de tun electronic şi, cînd se atinge ionizarea maximă a mediului activ, derulează descărcarea electrică a impulsului de bază cu formarea plasmei.

Cuvinte-cheie: electrod, plasmă, autoionizare, descărcare electrică.

The paper solves the problem aimed at developing a dispositive – multichannel electrode that provides plasma in impulse formation and provokes the auto-ionization of the active media (without auxiliary dispositive) and the increase of its durability (in the absence of discharge channels destroy). The developed electrode executes double function: it serves initial as an electron gun and, when the active media becomes maxim ionized, it manages the electrical discharge of the base impulse accompanied with plasma formation.

Keywords: electrode, plasma, auto-ionization, electrical discharge.

INTRODUCERE

Cea mai simplă şi răspîndită metoda de căpătare a plasmei de temperatură joasă este descărcarea în gaze.

Pentru cercetarea fenomenelor ce ţin de descărcarea electrică în gaze se foloseşte o construcţie alcătuită din doi electrozi, incluşi într-o cameră, aşezaţi la un anumit interstiţiu în care se află mediul gazos la diferite valori ale presiunii acestuia.

Fenomenul descărcăii electrice în gaze totdeauna începe cu străpungerea gazului. Dacă la electrozi se aplică o tensiune nu prea mare (~ 10V) nici un fel de efect de formare a plasmei în gaz nu va avea loc (curentul de scurgere este foarte mic ~ 10^{-15}A). Este cunoscut faptul că în aier la condiţii normale în lipsa cîmpului electric există ~ 10^3 perechi de ioni într-un cm^3. Străpungerea are loc în cazul, cînd în mediul gazos există un număr impunător de particule încărcate care apar ca rezultat al unor cauze aleatoare sau sub acţiunea unei surse permanente aplicate pentru stimularea procesului, de aceia iniţial descărcarea în gaze are caracter neautonom, însă dacă cîmpul atinge o careva valoare limită descărcarea capătă un caracter autonom care are loc sub acţiunea cîmpului electric.

Sub acţiunea cîmpului electric gazul se ionizează. Ionizarea are loc pe contul ciocnirii electronilor acceleraţi în cîmp electric cu moleculele neutre. Deci pentru aceste condiţii în gaz apare o avalanşă de particule încărcate, deoarece în procesul de ionizare participă noii electroni aparenţi ca rezultat a ionizării. Aşa un proces de ionizare în lanţ cu formarea noilor electroni liberi poartă denumirea de avalanşă electronică. Acest proces decurge foarte rapid şi ionizarea gazului capabil să conducă curentul prin el are loc în decurs de timp de la 10^{-7} – 10^{-3} s. Parcursul de mai departe a procesului de descărcare în gaze este funcţie de un şir de condiţii. Variaţia acestor condiţii permite de a obţine diferite tipuri de descărcari electrice în gaze: luminiscentă, sub formă de arc, sub formă de scîntei şi sub formă de coroană.

Pentru descărcarea luminiscentă este caracteristic formarea de straturi luminoase şi întunecate fiecare dintre care au denumirea sa.

Cunoaţterea legităţilor de formare a plasmei în medii gazoase este necesară pentru dezvoltarea de noi tehnologii cu aplicarea plasmei în calitate de sursă concentrată de energie.

Dezvoltarea noilor tehnologii este imposibilă în lipsa cunoaţterea proceselor de intervenţie a plasmei cu suprafeţele corpurilor de lucru în vederea conferii acestora de noi proprietăţi funcţionale permanente sau temporare.

Cel mai important aport al electronicii cuantice în spectroscopie îl prezintă studiul stărilor excitate oscilator a moleculelor poliatomice. Pentru atingerea acestui scop au

fost efectuate un şir de experimente referitor la excitarea de rezonanţă a moleculelor poliatomice aplicîndu-se diversele metode de excitare a lor. Excitarea poliatomică s-a transformat într-o metodă eficientă de cercetare a nivelelor de populare înaltă a moleculelor. Descrierea calitativă a excitărilor poliatomice a cerut un studiu al spectrelor de tranziţie oscilatorie a moleculelor cu populare înaltă energetică care a dus la apariţia unei direcţii noi şi anume spectroscopia moleculelor. La momentul există atît cantitativ cît şi calitativ baza proceselor fotofizice şi celor fotochimice care au loc în moleculele poliatomice aflate într-un cîmp electric şi interacţiunea moleculelor cu el la rezonanţă. Aşa procese prezintă în primul rînd o interacţiune neliniară a modei de rezonanţă cu radiaţie infraroşie şi în al doilea rînd interacţiunea dintre modele oscilatorii între ele datorită anarmonismului. Ambele aceste procese sînt legate între ele şi stă la baza caracteristicii moleculei poliatomice în cîmpul electromagnetic.

Manevrînd cu presiunea, compoziţia gazului, dimensiunile şi configuraţia electrozilor, mărimea interstiţiului, intensitatea cîmpului electric şi curentul de descărcare se poate de dirijat în limite largi parametrii plasmei: temperatura particulelor încărcate, concentraţia, gradul de ionizare a plasmei, distribuţia particulelor excitate după gradele lor de libertate.

Orice gaz în condiţii normale rezprezintă un bun dielectric, deoarece viteza de formare în gaze a electronilor liberi şi ionilor din cauza radiaţiilor proprii este extrem de mică (de ordinul zecilor de electroni într-o secundă într-un cm^3 de volum gazos). Din cauza aceasta pentru formare în gaze a unui număr semnificativ de particule încărcate este necesar într-un mod sau altul de ionizat atomii sau molecule.

Ionizarea gazului poate fi efectuată folosind două metode principial diferite:

1) gazul se ionizează sub influenţa iradierii cu particule sau fotoni, energia cărora este mai mare decît potenţialul de ionizare a atomilor sau moleculelor. Aflîndu-se într-un cîmp electric căpătăm descărcare, numită neautonomă;

2) dacă în gazul care se află într-un cîmp electric particulele libere încărcate capătă de sinestătător energia mai mare decît potenţialul de ionizare, atunci obţinem descărcare autonomă.

Pentru formarea descărcării autonome (sau neautonome) volumetrice în impuls este necesară ionizarea preventivă a mediului activ.

Este cunoscută metoda de obţinere a plasmei la descărcarea electrică, în care mediului activ dintre doi electrozi i se conferă o anumită configuraţie şi se ionizează preventiv cu dispozitive auxiliare [1]. O altă modalitate de căpătare a plasmei se bazează pe construcţia lainerului cu multe fire conductoare [2]. Dezavantajul acestuia constă în faptul că, în rezultatul funcţionării acestui dispozitiv, are loc topirea şi vaporizarea firelor ce intră în componenţa lainerului (are loc distrugerea lor) ceea ce induce o durabilitate mică.

În lucrare se propune o construcţie nouă a unuia dintre electrozi care asigură obţinerea plasmei provocînd concomitent auto-ionizarea mediului activ (fără dispozitive auxiliare). Deoarece construcţia electrodului permite eliminarea efectului de distrugere a electrozilor, durabilitatea lui sporeşte considerabil faţă de celelalte construcţii existente.

CONSTRUCŢIA ŞI MODUL DE FUNCŢIONARE A ELECTRODULUI

În fig. 1 este prezentată construcţia de ansamblu şi în secţiune a electrodului-multicanal [4].

Construcţia electrodului-multicanal propus în lucrare este alcătuită din: un sistem de canale identice 1 conectate paralel între ele iar lungimea acestor canale de descărcare este determinată de diametrul acestor canale şi este cuprinsă între 1-1,5 m), iar diametrele canalului în limitele 0,3-0,5 mm, executate din cupru tehnic de marca M-3 pentru a le asigura acestora rezistenţa activă necesară egală; în scopul evitării străpungerii între canale acestea sunt izolate între ele cu un strat dielectric 2 cu grosimea de cca. 50-100 μm din sticlă de cuarţ, iar în scopul asigurării formării unui câmp electric echipotenţial la

capătul de lucru 3, acesta se execută sub formă de plan format din terminaţiile circulare a acestor canale, capetele opuse (libere) 4 ale acestor canale sînt conectate electric între ele prin lipire tare cu ultrasunet evitând prezenţa materialului izolator.

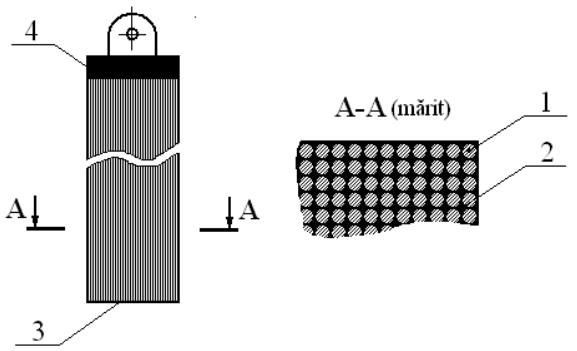

Fig. 1. Structura constructivă a electrodului-multicanal [4]:
1 – canale elementare; 3 – izolator; 3 – capul activ al electrodului-multicanal; 4 – borna de conectare

Electrodul-multicanal propus funcţionează în calitate de catod după cum urmează: la aplicarea unei diferenţe de potenţial în impuls, electrodul confecţionat serveşte iniţial în calitate de tun electronic, care sub acţiunea getului de electroni emişi provoacă ionizarea mediului de lucru – aer la presiune normală, iar când se atinge ionizarea maximă a mediului, automat şi neîntrerupt în timp, derulează descărcarea electrică a impulsului de bază şi în interstiţiul format de anod şi catod apare plasma descărcării electrice.

S-a stabilit experimental că, o aşa construcţie a electrodului-multicanal asigură pentru autoionizarea mediului activ cheltuielile energetice de ordinul 5-7 % din energia rezervată în bateria de condensatoare ($W_c=\frac{CU^2}{2}$) a generatorului de impulsuri de curent, schema electrică a căruia este prezentată în fig. 2.

Străpungerea dintre canalele acestui electrod este omisă şi prin aceia că ele reprezintă suprafeţe echipotenţiale pe întreaga lungime a electrodului.

Dispozitivul propus are terminaţiile capătului activ a electrodului elaborat care prezintă ascuţişuri (dimensiuni mici în raport cu suprafaţa plană a anodului), iar contra-electrodul prezintă o suprafaţă plană continuă, acesta sigură crearea între fiecare canal şi această suprafaţă a unui câmp electric E_1, de 1,5 ori mai mare în raport cu câmpul E pe care îl creează două suprafeţe plane continue şi prin acesta facilitează emisia electronică şi amorsarea descărcării electrice în impuls, acesta funcţionând la interstiţii 5…7 mm şi diferenţe de potenţial aplicate asupra lui de 25 kV.

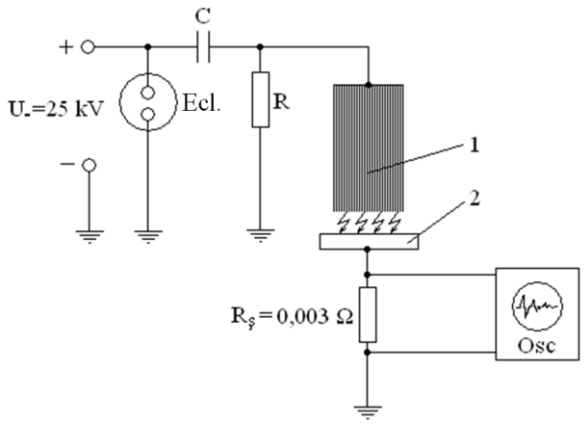

Fig. 2. Schema electrică principială a generatorului de impulsuri:
Ecl. – eclator, C – bateria de condensatoare,
R – rezistenţă de balast, Osc – osciloscop;
1 – electrodul elaborat; 2 – electrodul plat

Fiecare canal conductiv 1, în afară de rezistenţă activă R, posedă şi o anumită inductanţă L, determinată de diametrul şi lungimea lui, deaceea la suprafaţa de lucru a lui mai întîi apare diferenţa de potenţial aplicată, apoi prin aceste canale va trece un anumit curent, mărimea căruia este determinată de numărul total de canale şi energia rezervată în bateria de condensatoare. Curenţii care apar în canalele de descărcare electrică concurează între ei datorită rezistenţei active şi inductive a canalului (ωL), iar curentul total la descărcare este egal cu suma lor.

S-a demonstrat experimental că un aşa electrod-multicanal care funcţionează în regim de catod asigură obţinerea unui get de plasmă omogenă şi distribuită într-un volum considerabil de ordinul 1÷3 cm^3 pentru o durată de 0,25 μs (fig. 3).

Experimental s-a demonstrat că durata de funcţionare a electrodului-multicanal este practic nelimitată datorită distribuirii uniforme a câmpurilor electrice şi de temperaturi pe suprafaţa lui activă.

Fig. 3. Plasma descărcării electrice în impuls formată cu ajutorul electrodului elaborat

CONCLUZII

Analizînd cele expuse mai sus putem face următoarele concluzii:

1. Electrodul confecţionat îndeplineşte funcţie dublă: serveşte iniţial în calitate de tun electronic, iar când se atinge ionizarea maximă a mediului, automat şi neîntrerupt în timp, derulează descărcarea electrică a impulsului de bază cu formarea plasmei.
2. Străpungerea dintre canalele acestui electrod nu are loc datorită faptului că ele reprezintă suprafeţe echipotenţiale pe întreaga lungime a electrodului, curentul total al descărcării este egal cu suma curenţilor ce trec prin fiecare canal.
3. Electrodul-multicanal elaborat asigură obţinerea unui get de plasmă omogenă volumetrică în impuls (într-un volum de ordinul 1÷3 cm^3) pentru o durată de 0,25 μs.

BIBLIOGRAFIE

1. Королев Ю.Д., Месяц Г.А. Физика импульсного пробоя газов. – М.: Наука. Гл. ред. физ.-мат. лит., 1991, с. 93-115.
2. Устройство для получения высокотемпературной плазмы на основе многопроволочного лайнера. Патент Российской Федерации № 2222120. Дубинов А.Е., Сайков С.К., Селемир В.Д. 31.01.2002.
3. Велихов Е.П., Ковалев А.С., Рахимов А.Т. Физические явления в газоразрядной плазме: Учеб. руководство. М.: Наука, Гл. ред. физ.-мат. лит., 1987. 160 с.
4. Hirbu Arefa, Topala Pavel, Canţer Valeriu, Ojegov Alexandr. Electrod-multicanal destinat obţinerii plasmei prin descărcări electrice în impuls cu auto-ionizare. Cerere de brevet de invenţie. Nr. depozit: a 2013 0052. Data depozit: 2013.07.25.

Prezentat la redacţie la 1 octombrie 2013

CZU 621.771.06

SIMULAREA NUMERICĂ A PROCEDEELOR DE NETEZIRE ŞI DURIFICARE

Cosovschi P.
Universitatea Tehnică a Moldovei, bd. Ştefan cel Mare, 168, MD-2004, Chişinău, Republica Moldova
e-mail: c.pashag@gmail.com

Această lucrarea este destinată pregătirii complete a modelului supus simulării numerice pentru procesul de prelucrare prin metoda deformării plastice superficiale. Precizia şi discretizarea modelului pe elemente finite este necesară pentru obţinerea rezultatelor corecte şi practicabile.
Cuvinte-cheie: simularea numerică, discretizarea modelului, deformarea plastică superficială, elemente finite.

This paper is intended to a full preparation of a model subjected to the numerical simulation of the process of machining by surface plastic deformation method. The accuracy and discretization of the model through the finite elements is necessary to obtain correct and practicable results.
Keywords: numerical simulation, model discretiyation, surface plastic deformation, finite elements.

INTRODUCERE

Codul numeric folosit pentru simulare, LS-DYNA, este un program de analiză a proceselor şi fenomenelor fizice, cu largi posibilităţi de utilizare în domeniul mecanicii corpurilor deformabile. Ca metodă de analiză s-a optat pentru o metodă cu reţea – metoda elementelor finite - care asigură o foarte bună reprezentare discretă a corpurilor implicate în proces. Solverul explicit al programului LS-DYNA, ales pentru integrarea ecuaţiilor, are avantajul unei mai bune reprezentări în timp a soluţiilor, faţă de solverul implicit. Alegerea este justificată de faptul că procesele analizate sunt procese mecanice de durată, continue şi se produc cu o anumită viteză. Pentru o soluţie corectă şi completă este necesar ca incrementul de calcul să fie în concordanţă cu pasul reţelei şi cu viteza relativă dintre semifabricat şi sculă.

Conform metodologiei, pentru realizarea simulării numerice a proceselor de netezire şi durificare a sculelor prin deformare plastică superficială este necesară realizarea unui model discretizat cu elemente finite în concordanţă cu scopul urmărit.

Discretizarea modelului fizic ca o esenţializare a procesului impus analizei, a fost realizată cu densităţi foarte diferite de elemente finite, în funcţie de locul şi importanţa corpului în proces. Modelul procedeului de netezire şi durificare a sculelor prin deformare plastică prin contact de alunecare este reprezentat în Fig. 1.

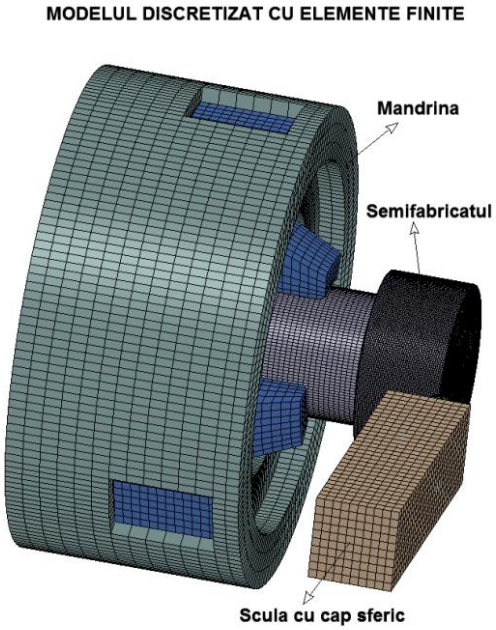

Fig. 1. Modelul discretizat cu elemente finite

Corpul cel mai important în ansamblu – semifabricat – a fost discretizat diferenţiat cu 142848 elemente finite SOLID cu 8 noduri şi un număr total de noduri de 156369, aşa cum se arată în Fig. 2. Stratul superficial al semifabricatului, locul în care se produc defromaţiile plastice are cea mai mare densitate de discretizare. Astfel, pe generatoarea suprafeţei prelucrate sunt dispuse 64 de elemente cu pasul de 0.25 mm iar pe circumferinţă sunt 256 de elemente cu pasul de 0.43 mm. Reţeaua diferenţiată de elemente finite, reprezentată în Fig. 3, a redus considerabil efortul de calcul.

Fig. 2. Semifabricatul cilindric discretizat cu elemente finite

Sfericitatea corpului sculei a fost asigurată cu precizie suficientă prin modelarea pe suprafaţa activă cu o reţea fină cu pasul de 0.4 mm.

Pentru celelalte corpuri ale modelului reţeaua de discretizare este mai lejeră, dar suficient de densă pentru a asigura simularea corectă a funcţionării, mai ales a contactelor la prinderea piesei de prelucrat şi la ghidarea bacurilor. În total, pentru discretizarea întregului model, au fost folosite 224512 de elemente finite 3D de tipul SOLID cu 8 noduri şi un număr de 261264 de noduri. Această schemă de discretizare a fost folosită fără modificări, la toate formele de semifabricate.

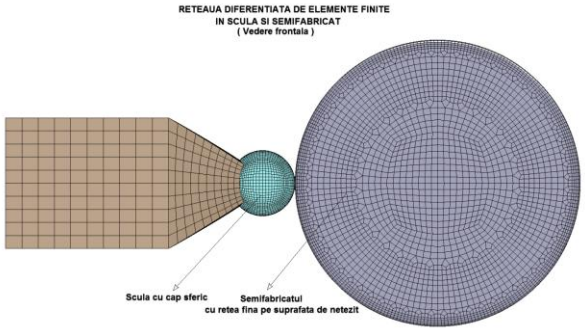

Fig. 3. Reţeaua diferenţiată de elemente finite în sculă şi semifabricat

Procedeul de netezire presupune că suprafaţa de prelucrat are o rugozitate produsă prin procesul tehnologic de fabricaţie, cel mai frecvent prin aşchiere.

Modelele analizate încearcă să fie fidele realităţii, purtând pe suprafaţa de prelucrat o rugozitate simulată, similară celei rezultate în procesul de strunjire normală, cu avansul compatibil cu reţeaua de elemente finite, de 0.5 mm/rot.

Generarea rugozităţii virtuale s-a realizat cu o metodă de calcul aleator. Astfel, nodurile de pe suprafaţa de prelucrat a piesei au fost deplasate aleator în toate cele trei direcţii, folosind un parametru al generării cu o valoare impusă în acord cu rugozitatea dorită. Cu ajutorul parametrului generării se delimitează câmpul probabilităţii uniforme. Pentru cele trei direcţii deplasările impuse nodurilor s-au calculat cu următoarele relaţii aleatoare:

- direcţia radială: $\Delta_r = \pm D[1\text{-}RAND(-1, 1)]$,
- direcţia circumferenţială, ca deplasare unghiulară: $\Delta_t = D \cdot RAND(-1, 1) \cdot 180°/\pi R$, (1)
- direcţia axială: $\Delta_a = 5 \cdot D \cdot RAND(-1, 1)$,

în care RAND(-1,1) este un număr real, extras aleator, cu densitate de probabilitate uniformă, din intervalul (-1, +1), iar R este raza medie a suprafeţei înainte de alterare.

Rugozitatea fictivă corespunzătoare procedeului de strunjire normală R_a = 3.2 ...6.3 μm se obţine pentru un parametru de generare Δ = 0.01 mm. În lucrare se utilizează mai des rugozitatea măsurabilă R_z. Concret, pentru parametrul de generare folosit, Δ = 0.01 mm, valorile rugozităţii R_z sunt în jur de 20 μm şi are corespondentul $R_a \approx 5$ μm, încadrat în limitele impuse.

Evidenţierea clară a unora dintre efectele procedeului – netezirea suprafeţelor – a implicat realizarea unor modele cu rugozitate vizibilă şi măsurabilă virtual, ca cel din Fig. 4.

Modelarea suprafeţelor cu rugozităţi mai mici, cu $R_a < 3.2$ μm, ar conduce la discretizări cu un număr mult mai mare de elemente şi practic, la imposibilitatea soluţionării cu un efort de calcul rezonabil.

Evaluarea rugozităţii generate aleator pe o suprafaţă (Fig. 4) a fost făcută, utilizând procedura standardizată, prin calcul într-o serie de noduri predefinite, dispuse pe generatoarea suprafeţei. Astfel, pentru piesa cilindrică reprezentată in Fig. 4 s-a obţinut seria de valori: 20.15, 19.28, 17.23, 19.22, 21.65 μm, cu valoarea medie R_z = 19.5 μm.

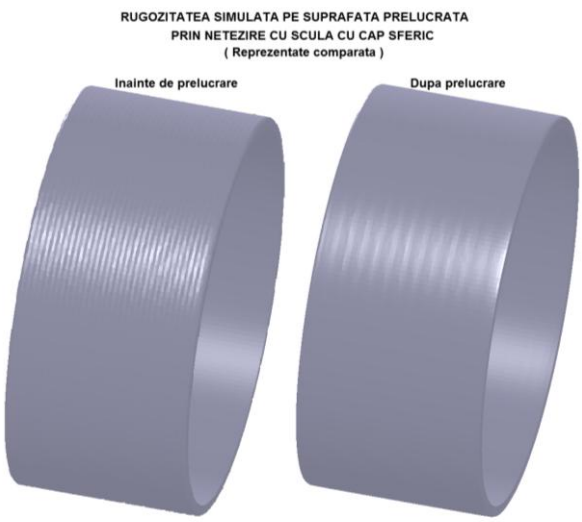

Fig. 4. Rugozitatea simulată pe suprafaţa prelucrată prin netezire cu scula cu cap sferic

După prelucrare, rugozitatea va fi recalculată în aceleaşi noduri de control şi comparată cu cea iniţială. Din considerentele expuse mai sus, derivă justificarea utilizării sculei cu capul de netezire sferic cu rază mare R_{sf} = 4 mm, la limita celor uzuale.

Controlul forţelor aplicate de sculă piesei în procesul de prelucrare simulat este realizat de sistemul de senzori dispuşi pe corpul sculei.

Al doilea pas important în faza de pre-procesare se referă la formularea modelului de material. Analiza consistentă a materialelor asociate modelelor simulate făcute îşi dovedeşte acum utilitatea. Modelul de plasticitate Johnson-Cook sub formă simplificată

$$\sigma_y = \left(A + B\varepsilon_p^n\right)\left(1 + C\ln\frac{\dot{\varepsilon}_p}{\dot{\varepsilon}_0}\right)$$

are reprezentarea cea mai completă. Termenul termic din relaţia, din motive justificate – încălzire nesemnificativă, dovedită experimental – a fost suprimat.

Pentru fonta cenuşie cu grafit lamelar, folosită în simulare, valorile coeficienţilor A, B şi n sunt cele determinate experimental. Coeficientul C a fost preluat de la materiale similar cu valoarea C = 0.06, conform pct. 1 din lucrare.

Celelate corpuri sunt modelate cu materiale elastice (oţeluri) sau perfect rigide.

Condiţiile pe frontiere şi funcţionale simulate au fost stabilite în concordanţă cu parametrii proceselor tehnologice de netezire şi de durificare.

Prinderea piesei în madrină este simplă, prin contact între bacuri şi prelungirea tehnologică a piesei.

Contactul între capul sferic a sculei şi semifabricat se realizează fie elastic, cu controlul forţei, fie rigid, cu controlul deplasării. Avantajele şi dezavantajele acestor două posibilităţi de control se vor analiza după simulările numerice.

Turaţia, avansul longitudinal, forţa de apăsare sau adâncimea radială sunt stabilte conform criteriilor generale.

Materialul supus prelucrării simulate – fontă cenuşie cu grafit lamelar cu duritate Brinell, determinată experimental, cuprinsă între 122 şi 140 HB şi, în consecinţă datele au fost folosite cu valoare orientativă.

Densitatea mică şi rugozitatea mare (3.2...6.3 μm) specifică fontei cu grafit lamelar, dar şi riscul de producere a fărâmiţării superficiale a materialului, au influenţat decisiv alegerea parametrilor regimului de lucru.

Raza aleasă pentru capul sferic, R_{sf}=4 mm, se poate justifica extrapolând tendinţele. Conform acestor tendinţe, pentru materiale moi, cu densităţi mici şi rugozităţi mari, pentru realizarea efectului sunt necesare scule cu raze mai mari.

Viteza periferică a suprafeţei de prelucrat stabilită pentru simulare este puţin inferioară limitei minime, recomandate. Cauza principală care a impus o viteză periferică la limita inferioară descrisă a fost disponibilitatea unui agregat dotat cu un sistem dinamometric cu 6 grade de libertate pentru probele experimentale, care funcţionează optim la turaţia de 380 rot/min. Agregatul respectiv se găseşte în laboratoarele Facultăţii de Ingineria şi Managementul Sistemelor Tehnologice din cadrul Universităţii POLITEHNICA Bucureşti.

Necesitatea confruntării soluţiilor simulate cu datele experimentale a condiţionat alegerea vitezei periferice corespunzătoare acestei turaţii (≈ 42 m/min). Turaţia mică a arborelui utilajului este un dezavantaj deoarece măreşte durata calculului unui ciclu tehnologic complet.

În consecinţă simulările importante au fost realizate la turaţia de 380 rot/min.

Valoarea avansului axial pentru majoritatea simulărilor (s = 0.09 mm/rot) se încadrează în recomandările.

Pentru forţele de apăsare s-a folosit o gamă mai largă cuprinsă între 200 şi 1000 N. Forţele mai mari sunt necesare pentru netezirea rugozităţilor mai mari (6.3 μm).

Când se doreşte durificarea în stratul superficial forţele de apăsare radială trebuiesc crescute.

În procedeul cu sculă rigidă – controlul în deplasări – adâncimea de pătrundere a fost reglată în funcţie de efectul dorit, încadrându-se în limitele impuse h_d=0.03...0.3 mm.

Utilajul experimental disponibil lucrează cu sculă rigidă dispusă pe dispozitivul dinamometric. Are utilizare limitată la suprafeţe cilindrice coaxiale.

Un agregat experimental complet pentru aplicarea procedeului cu sculă rigidă este mai greu de realizat deoarece necesită un sistem central activ care să urmărească continuu poziţia sculei în raport cu suprafaţa de prelucrat.

De notat că dispozitivul tehnologic simulat este complet izolat şi nu interacţionează cu alte corpuri, fiind o idealizare a unui agregat experimental, care în întregul lui, prin deformatii elastice, jocuri şi vibraţii, influenţează calitatea produsului.

CONCLUSION

Codul numeric contemporan dă posibilitatea de a analiza procesele şi fenomenele fizice în domeniul mecanicii corpurilor deformabile. Acestea ne dau posibilităţi, esenţial de a optimiza procesele de proiectare. Staţiile contemporane şi puternice pot prelucra un volum extrem de mare de informaţii pentru fiecare element finit solid. Este de folos aplicarea descritizării diferenţiale. În caz de faţa cel mai important corpul – semifabricat a fost descritizat la 142848 elemente cu 8 noduri şi un număr total de noduri de 156 369. Lucrarea dată a confirmat practibilitatea folosirii acestei metode de proiectarea proceselor tehnologice şi obţinerea informaţiei necesare la etapele iniţiale pentru optimizarea experementelor complicate şi costisitoare.

BIBLIOGRAFIE

1. Balakşcin B. C. Teoria i practika tehnologhii maşcinostroenia: V 2-c kN. – M.: Maşcinostroenie, 1982 - 218 kn. 2. Osnovî tehnologhii maşcinostroenia. 1982. 367 s.
2. Balter M. A. Uprocnenie detalei maşcin M.: Maşcinostroenie. 1978. 184. s.
3. Barabici M. B., Horujenko M. V. Nakatîvanie ţilindriceskih zubceatîh kolios. - M.: Maşcinostroenie, 1970. 218 s.
4. Belov V. A. Tehnologhia obrabotki ploskostei poverhnostnîm deformirovaniem /Pod red. A.A. Matalina, - Kiev: Tehnika, 1972. 125 s.
5. Berştein M.L., Zaikovskii V. A., Kaputkina M, L. Termomehaniceskaia obrabotka stali. M.: Metallurghia. 1983. 480 c.
6. Boiţov A.G. i dr. Uprocnenie detalei kombinirovannîmi sposobami /A.G. Boiţov, V.N. Maşkov, V.A. Smolenţev i dr. M.: Maşcinostroenie, 1991. 144 s.
7. Boiţov A.G., Maşkov V.N., Smolenţev V.A., Hvorostuhin L. A. Uprocnenie poverhnostei detalei kombinirivanîmi sposobami. M.: Maşcinostroenie, 1991. 144 s.

Prezentat la redacţie la 5 octombrie 2013

CZU 621.9.048.4

MICRO-OXIDATION OF SILICON SURFACES BY MEANS OF ELECTRICAL DISCHARGES IN IMPULSE

Topala P.[1*], Melnic V.[2], Guzgan D.[1]
[1]Alecu Russo Balti State University, 38 Pushkin Str, MD-3100, Balti, Republic of Moldova
[2]Technical University of Moldova, 168 Stefan cel Mare Blvd., MD-2004, Chisinau, Republic of Moldova
*e-mail: pavel.topala@gmail.com

Articolul prezintă rezultatele strudiul teoretico-experimental privind formarea peliculelor de oxizi pe suprafeţele din siliciu cu ajutorul oxidării termice rapide în plasma cauzată de descărcările electrice în impuls. Procesul de oxidare a fost obţinut în atmosferă în condiţii normale. Se arată că proprietăţile peliculelor de oxizi depind de puterea disipată pe suprafaţa prelucrată, precum şi de materialul de bază a electrozilor.

Cuvinte-cheie: descărcare, oxidarea suprafeţelor din siliciu, pelicule de oxizi.

The paper presents the results of the theoretical and experimental study of the formation of oxide films on silicon surfaces by means of rapid thermal oxidation in plasma caused by electrical discharges in impulse. The oxidation process has been carried out under normal atmospheric conditions. It has been shown that the properties of the oxide films depend on the processing power as well as the electrode base materials.

Keywords: discharge, oxidation of silicon surface, oxide films.

INTRODUCTION

Oxidation is a chemical reaction between metal or semiconductor and an oxidizing agent (oxygen, ozone, water, carbon dioxide, etc.). The purpose of the oxydation of the samples surfaces of conducting [6] and semiconducting materials is the formation of protecting pellicles resistant to corrosion having high electrical resistivity, various radiation absorbability properties, etc. In a particular case of the oxidation of silicon samples the observed result was the formation of SiO_2 layer having dielectric and shielding properties determined by the process of adding controlled impurities. The SiO_2 structure is used as an insulating layer to separate different parts of the integrated circuit. By preserving semiconducting properties of the processed part, the technology of oxide films production on the semiconducting materials is very important since by preserving semiconducting properties of the processed part, it enables the wide use of these materials as the building elements in the electronics and microelectronics engineering industry. The formation of thin layers of SiO_2 on the silicon samples is fundamental for the concepts of constructional design and the technology of silicon devices for integrated circuits and nanoelectronic equipment [1].

Silicon oxidizes under the ambient temperature, in the atmosphere with oxygen content. But after the oxide layer reaches the depth of the 2-3 atomic layers, the layer grow stops. This phenomenon is explained by the the oxide layer protecting the silicone against its own further oxidation. In order to obtain the necessary depth of oxidized layers, the oxidation phenomenon is further activated by the temperature increase [4-5].

Folowing the classification [1], the methods of the silicon oxide layers formation can be divided into 2 basic groups. The first group includes methods based on the formation of oxidized pellicles by means of deposition from the outside. In other words the silicon piece plays the role of a nonreactive substrate. The second group contains the methods of direct oxidation of the silicon sample surface, when the oxide films are formed from the material of the subtrate by means of chemical interaction. Thermal oxidation of silicon is a very common technological approach, it is widely practiced in industry.

For the formation of oxide pellicles the following approaches are used:

- thermal oxidation in the presence of oxygen, called *dry oxidation* [1];

- thermal oxidation in the presence of oxygen and water vapour, called *wet oxidation* [1];
- thermal oxidation in the presence of only water vapour, called *steam oxidation* [1];
- oxidation by electrochemical means, called *anodic oxydation* [1];
- oxidation with the help of oxygen plasma, called the *oxidation in plasma* [4,5].

Often combined approaches are used.

The classical method of the silicon oxidation is thermal oxidation, performed by means of placing the processed material into a special furnace, so that to provide the diffusion and thermal oxidation in the oxidic medium. Under these conditions the oxygen contained in the oxidic medium reacts with the surface of the processed sample, heated and maintained in a certain thermal mode for a certain period of time in the furnace. Dry or wet (with water vapour) oxygen is used as an oxidic medium. The process of the sillicon oxidation is usually realized within the temperatures of 800-1300°C. This method requires a considerable energy and time consumption.

The oxidation in plasma may find a larger applicability due to the fact that the process of silicon oxidation occurs in a more intensive way in comparison to the „classical" oxidation.

The plasma for this approach can be obtained by two means:

- by the RF-discharge (microwave discharge);
- by the electric glow-discharge with a direct current.

The main purpose of the superficial oxidation of the sample by applying electric discharges in impulse (EDI) is the change in the properties of the surface layer of the sample, which is exposed to thermal or chemithermal processing in the plasma channel inside the interelectrode gap. In other words it provokes the activation of the processed surface (by means of heating, bombardment of ions, light emission, high-intensity electrical fields, etc.) And owing to the ionization of the components from the processing oxidizing medium and their acceleration in the electric field of the electric discharge there occurs its intrusion into the processed surface causing the change of material structure and thus of the layers properties [3].

THEORETICAL PREMISES AND METHODOLOGY OF EXPERIMENTAL INVESTIGATIONS

It is important to underline that the experimental investigations were performed in the normal pressure conditions at the indoor temperature. For the realization of the experimental investigations concerning the processing of semiconductor surfaces by applying the EDI plasma a special equipment was used: the electrical block-scheme of which is shown in Fig.1.

The equipment consisted of the following main parts: the block of power pulses which is a generator of RC-type pulses (G), the block of inducing (BI) and the block of command (BC). The command unit allows fine adjustment of the pulse repetion frequency within 1-300 Hz. The principle of the generator operation is based on the accumulation of a certain amount of the electrical energy in the capacitor battery and its discharging into the interelectrode gap in a short-time impulse (τ = 220 ms).

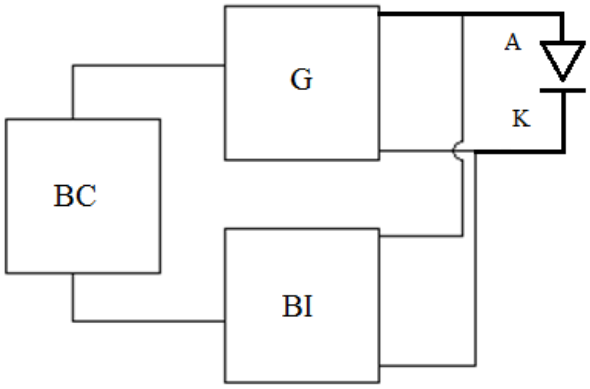

Fig. 1. The main electrical block-scheme of the equipment:
BC – block of command; G – RC-type pulse generator; BI – block of inducing

At the moment of piercing the interstice the electrons drawn from the cathode surface turn towards the anode. The electrons are accelerated in the interstice electric field, they collide with gas molecules and atoms in the

interstice and produce the ionization of the working medium [2]:

$$O_2 \rightarrow O^+ + O^+ + 2e^-;$$
$$O_2 + O^+ \rightarrow O_3^+, \text{ etc.} \quad (1)$$

The dissociation and recombination of the interstice medium take simultaneously:

$$O_2 + 2e^- \rightarrow O^- + O^-;$$
$$O_2 + O^- \rightarrow O_3^-; \quad (2)$$
$$O^+ + O^- \rightarrow O_2;$$
$$O^+ + e^- \rightarrow O, \text{ etc.}$$

Thus the plasma channel formed in the interelectrode gap contains positive oxygen ions, which move to the processed sample surface under the action of electrodynamic force. Owing to this fact the activation of the semiconductor surface occurs, that causes its oxidation and difusion of the environment elements in the depth of the sample.

There are following reactions taking place on the silicon sample surface [5]:

$$Si + O_2 \rightarrow SiO_2 \quad (3)$$
$$Si + 2H_2O \rightarrow SiO_2 + 2H_2.$$

In order to achieve the proper energetic balance necessary for the formation of the oxidized layer caused by interaction of plasma channel with the sample surface it is to follow certain conditions: the energy density of the processed surface must be less than specific heat fusion of the sample material [3]:

$$Q = \frac{4W_S}{\pi d_c^2 S} < Q_{top}, \quad (4)$$

Q – is the energy released in the interelectrode gap, Q_{top} – specific heat fusion of the processed material $Q_{top} = q\rho$. The energy released in the interstice is one accumulated in the capacitor bank of the generator, taking into account η – its degree of efficiency in the interstice.

$$W = \frac{CU^2}{2}\eta. \quad (5)$$

A range of experimental investigations were carried out using various dimensions of the interstice and charging voltage of the generator of RC-type impulses, that is varying the energy of the electric discharges in impulse, Fig. 2.

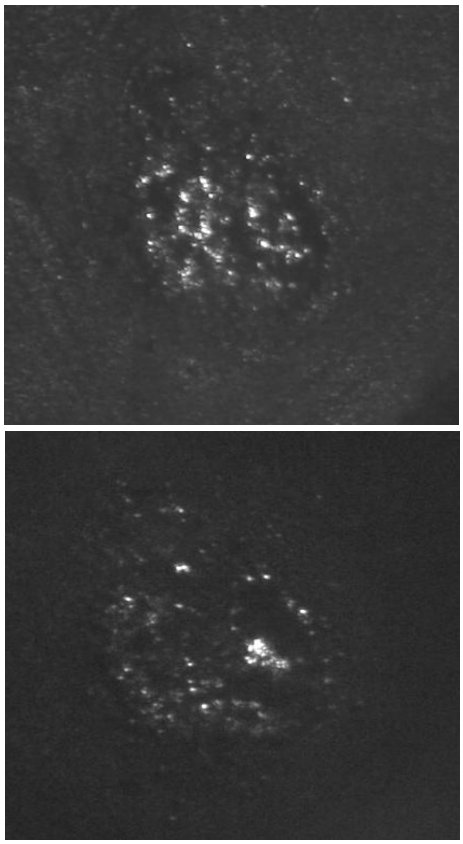

a)

b)

Fig. 2. Sample surface (sample-cathode) after processing EDI with tungsten electrode:
C = 8 μF, f = 16 Hz:
a) S = 1 mm, U = 100 V; b) S = 1,2 mm, U = 100 V

There are to observe erosion craters after the EDI processing of the sample connected in a traditional way into the circuit of the RC-type pulse generator, in the capacity of cathode. This fact attests that the appliance of the inductive impulses leads to the electrical breakdown of the semiconductor and results in the loss of the semiconductor properties. This effect occurs due to the excessive heating of the processed surface accompanied by melting, partial vaporization and uncontrolled solidification (in amorphous state) of the processed semiconductor.

For this reason there was designed and developed a technological scheme, which provides the formation of the oxide films on the semiconductor surface by means of EDI with indirect application (as presented on the Fig. 3).

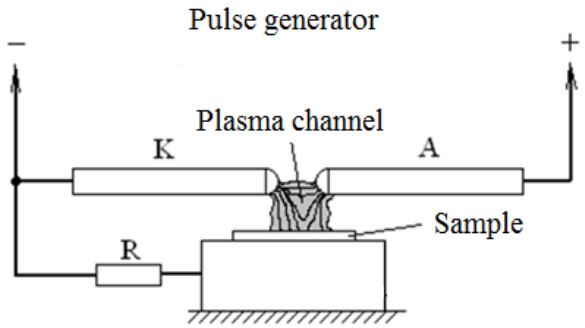

Fig. 3. Technological scheme of processing the semiconductor sample surface with indirect application of the plasma channel

For a precise control of the energetic mode the basic electrodes were sharpened cone-wise having 90º tip angle. Due to the fact that the processed semiconductor is connected into the discharge circuit by means of active resistance (R) of the MΩ order, the plasma channel resulting from the electric discharge between the basic electrodes, partially contacts with the sample surface changing its properties allowing to avoid its breakdown.

In the process of the experimental investigations the interstice size between the basic electrodes constitues $S_{e.b.}$ = 2mm, and the distance between basic electrodes and sample: $S_{e.s.}$ = 1,5mm. The material of the processed sample – Si (100).

THE RESULTS OF EXPERIMENTAL INVESTIGATIONS AND THEIR ANALYSIS

The processing of the semiconductor by means of EDI plasma according to the scheme presented on the Fig. 3 results in the formation of thin layer of oxide on its surface. The annealing colours appearing on the processed sample surface after the indirect application of EDI plasma prove that the oxide films were really formed (a dark brown layer).

The morphology of the semiconductor sample surface oxidized in the result of the EDI plasma application is presented on the Fig. 4 and 5.

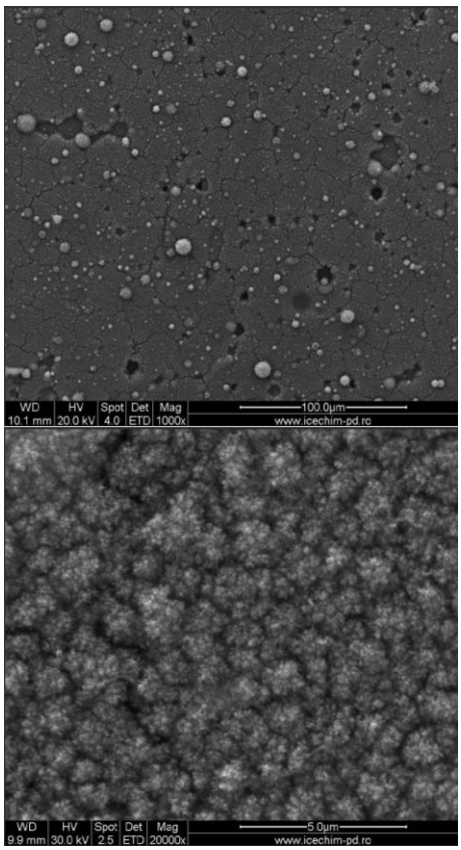

Fig. 4. The morphology of the semiconductor sample surface after the superficial oxidation applying plasma: the material of the basic electrodes – steel with low content of carbon; U = 100V; C = 100µF

The SEM analysis of the obtained films affirms that it essentially depends not only on the energetic conditions of processing, but also on the material of the basic electrodes. Thus we can state that usinng the steel electrodes results in the more pronounced and non-uniform structure of the oxide layer. The use of tungsten basic electrodes allows to obtain thiner and more uniform structure of the oxide films.

CONCLUSIONS

- the oxidation of surfaces by application of electrical discharges in impulse can be performed under the normal pressure conditions at the indoor temperature;
- the processed sample must be connected to the discharge circuit in the capacity of cathode by means of a resistance of the MΩ order;
- the morphology of the obtained pellicles depend on the energetic conditions of processing and on the material of the basic electrodes.

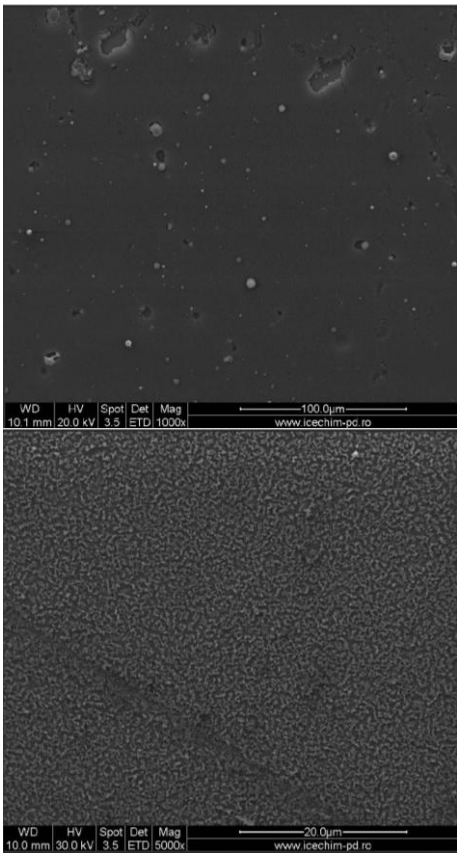

Fig. 5. The morphology of the semiconductor sample surface after the superficial oxidizing by application of plasma: the material of basic electrodes – W; U = 120V; C = 100µF.

BIBLIOGRAPHY

1. Физико-химические основы технологии электронных средств / Сост. В. И. Смирнов. – Ульяновск: УлГТУ, 2006. 22 с.

2. Topala P. Physico-chemical effects provoked in the piece surfaces during machining by applying electrical discharges in impulse. Proceedings of the 15th International Conference „Modern Technologies, Quality and Innovation", ModTech 2011 – New face of T.M.C.R., 25–27 May, 2011, Vadu lui Vodă, Republic of Moldova. Ch., 2011. Vol.2, p. 1097-1100.

3. Topala P., Stoicev P. Tehnologii de prelucrare a materialelor conductibile cu aplicarea descărcărilor electrice în impuls, Tehnica Info, Chişinău, 2008. 265 p.

4. Hess D.W. Plasma-assisted oxidation, anodization and nitridation of silicon / IBM Journal of Research and Development. – 1999. Vol. 43, №1/, p. 127–146.

5. Sayed-Masoud Sayedi. Experimental investigations of corona-discharge oxidation of silicon. Thesis (Ph.D.) Concordia University, 1997. 358 p.

6. Topală P., Ojegov A. Formation of oxide thin pellicles by means of electric discharges in pulse. Annals of the Oradea University. Fascicle of management and technological engineering, volume VII (XVII), 2008. CD-ROM Edition. Editura Universităţii din Oradea, România. ISSN 1583-0691, CNCSIS „Clasa B+", p. 1824-1829.

Prezentat la redacţie la 8 octombrie 2013

CZU 621.9.048.4

OXIDE NANOMETRIC PELLICLES FORMATION BY APPLYING ELECTRICAL DISCHARGES IN IMPULSE

Topala P.[1*], Stoicev P.[2], Ojegov A.[1]
[1]Alecu Russo Balti State University, 38 Pushkin Str., MD-3100, Balti, Republic of Moldova
[2]Technical University of Moldova, 168 Stefan cel Mare Blvd., MD-2004, Chisinau, Republic of Moldova
*e-mail: pavel.topala@gmail.com

Articolul prezintă rezultatele cercetărilor teoretice şi experimentale privind fenomenele ce se produc în procesul formării peliculelor nanometrice de oxizi şi hidroxizi cu aplicarea descărcărilor electrice în impuls (DEI). Analiza compoziţiei chimice a suprafeţei prelucrate (EDX – Energy Dispersive X-ray analysis) atestă prezenţa oxigenului care atinge pînă la 60% at. pentru suprafeţele din oţeluri, 30-35% at. pentru cele din aliajele titanului, pînă la 20% at. pentru cele din aliajele aluminiului şi pînă la 50% at. pentru cele din aliajele cuprului. Prezenţa în volum considerabil a azotului a fost depistată numai în aliajele titanului şi fierului (şi constituie aproximativ 15% at.), pe cînd în aliajele alumiului şi cuprului prezenţa lui este neînsemnată. Analiza fazică superficială (XPS - X-ray Photoelectron Spectroscopy) a oxigenului ne-a permis să constatăm că oxigenul în peliculă formează trei compuşi (structuri) $-O^{-2}$ (oxid), - OH^- (hidroxid), şi structure organice de tipul O-C şi O-C=O. Analiza chimică a arătat că concentraţia fiecărei dintre aceste trei componente constituie 0,89:1,00:0,50.

Cuvinte-cheie: descărcări electrice în impuls, peliculă de oxid, pată electrodică „rece”, microduritate, rugozitatea.

The paper presents the results of theoretical and experimental investigations of phenomena that accompany the formation of nanometer oxide and hydroxide pellicles by applying electrical discharges in impulse (EDI). The chemical content of processed surface analysis (EDX – Energy Dispersive X-ray analysis) attests the presence of oxigen that reaches up to 60% at. for steel surfaces, 30-35% at. for those made of titanium alloys, up to 20% at. for those made of aluminum alloys, and up to 50% at. for those made of copper alloys. The presence of considerable amounts of nitrogen is found only in titanium and iron alloys (and constitutes about 15% at.), while in aluminum and copper alloys its presence is not significant. The superficial phase analysis (XPS - X-ray Photoelectron Spectroscopy) of the oxigen allowed us to state that the oxigen in pellicle forms three base compounds (structures): $-O^{-2}$ (oxide), - OH^- (hydroxide), and organic structures of the type O-C and O-C=O. The chemical analysis showed that the concentration of each of the three components is 0.89:1.00:0.50.

Keywords: electrical discharges in impulse, oxide pellicle, "cold" electrode spot, micro-hardness, roughness.

INTRODUCTION

Oxidation of metal surfaces has found applications in various fields of technology for corrosion protection [9] and to change the electrical properties of surfaces in electrical and radio engineering [6, 7].

For this purpose, the method of electrolytic deposition of thermodynamically stable pellicles on some metal surfaces is applied, which can be obtained only at the so-called fed metals, which include aluminum, titanium, tantalum, niobium, etc. The spark-anodic electrolysis, also known as micro-plasma or micro-arc oxidation, has been developed [2, 3].

Depositions formed by this method are a large range of structural, technological and operational requirements: micro-hardness, wear resistance, low coefficient of friction, and ability of electro-isolation, erosion resistance, and high adhesive properties. An important advantage of such depositions is that their properties are of complex operational character.

Low-alkaline and acidic electrolytes and metal salt solutions are used to realize this process. Deposition properties depend on the chemical composition of the alloy, concentration, composition and temperature of the electrolyte, electrical regimes of the process and its duration, etc.

Coverings mainly consist of solid crystalline phases in the matrix of softer oxide phase of metals that form part of the alloy and the electrolyte. This structure provides a high micro-hardness, wear-proof and corrosion resistance, heat protection and electro-isolation properties of the covering.

The application of this technology implies the use of special devices for electrolytic processes and the adoption of measures required to ensure safe working conditions for staff.

From the moment of application the electrical discharges in impulse (EDI) for technological purposes in dimensional processing [11], in deposit formation of compact and powder materials [1, 5], the micro-metallurgical processes that occur in the surface layer of the work-piece in both liquid and solid phases were studied.

It has been established that the formation of new alloys in the processed surface is accompanied by convective mixing of the components in the liquid phase and the diffusion of elements in the substrate from the liquid phase of the deposition.

In the work [1] it has been shown that for the interstice greater than 0.03 mm, the interaction of EDI plasma channel with the processed surface is manifested by the appearance of an indent consists of a central zone that represents a crater with liquid phase and a heat-affected zone of freshly etched metal color.

For certain sizes of the interstice, the central zone disappears, and the processed surface represents only a heat-affected zone where phenomena of quenching and enriching piece material with elements from the work media occurs.

Recently, a number of works [6-10] has been published where the results on the electro-discharge oxidation of metal surfaces under ordinary conditions are presented.
Coverings obtained by this method have usually a dual structure. It consists of an inner base layer on the edge of the metal-coating and external outer layer (coat).

The base layer is fine-porous, has a crystalline structure and constitutes 60…90% of the covering thickness. The outer layer coating is less hard, more porous, has an amorphous structure and takes on the 40…10% of the thickness.

The coating under the oxidation process is able to germinate in metals in about 10 to 60% of the total thickness of the coating in the depth and consists mainly of oxides of the elements contained in the machined alloy and elements from the interstice.

The following chemical reactions are produced on the surface of the electrodes [10, 12]:

- on the anode:

$$\begin{gathered} xMe + yO^- \rightarrow Me_xO_y + (y-x)e^-; \\ xMe + yO^{3-} \rightarrow Me_xO_y + O_2 + (y-x)e^-; \\ xMe + yOH^- \rightarrow Me_x(OH)_y + (y-x)e^-; \\ xMe + yN^- \rightarrow Me_xN_y + (y-x)e^- \text{ and so on.} \end{gathered} \quad (1)$$

- on the cathode:

$$\begin{gathered} xMe + yO^+ + (y-x)e^- \rightarrow Me_xO_y; \\ xMe + yO^{3-} + (y-x)e^- \rightarrow Me_xO_y + O_2; \\ xMe + yH_2O + (y-x)e^- \rightarrow Me_x(OH)_y + \frac{y}{2}H_2; \\ xMe + yN^+ + (y-x)e^- \rightarrow Me_xN_y \text{ and so on.} \end{gathered} \quad (2)$$

EDI method allows to form coverings on pieces of complex shapes and of any configuration, including the internal surface of pipes [9].

The process operates at room temperature, which positively affects the constancy of the base metal physical properties.

The main characteristics of coverings formed by applying the EDI method are the following: layer thickness – up to 240 nm, micro-hardness – up to 2000 HV, approaches the hardness of corundum; surface roughness of coatings after oxidation – Ra = 0.05...0.10 μm.

The analysis of the operational properties of coatings obtained by EDI oxidation shows that these properties are closely related. Total thickness of covering, taking into account the number of electricity spent on it, demonstrates the high performance and efficiency of the process.

The boundary between the main piece material and covering relative to its original size is essential both for the adoption of constructive decisions on the use of pieces with EDI coverings and for the design of technological process of manufacturing such pieces.

METHODOLOGY OF EXPERIMENTAL INVESTIGATIONS

The main challenge for the stage of preliminary research of EDI coatings was to search for a technological regime of the oxidation that contributes to the formation of oxide pellicles with high operational properties on the pieces made of metallic materials and their alloys. The chemical content of machined pieces materials were taken into account during the EDI (table 1).

Table 1

Chemical content of machined pieces materials

Alloy	Chemical content
Iron alloy	
Steel 45 (C45)	0,42-0,50 % C; 0,17-0,37 % Si; 0,5-0,8 Mn; ≤0,25 % Cr; ≤0,04 % S; ≤0,035 % P; ≤0,25 Cu; ≤0,25 % Ni; ≤0,08 % As; the rest (basis) – Fe
Titanium alloy	
VT-8 (TiAl6Mo4)	5,8-7,0 % Al; 2,8-3,8 % Mo; ≤0,5 % Zr; 0,2-0,4 % Si; ≤0,30 % Fe; the rest (basis) – Ti
Aluminum alloy	
D16 (AlCu4Mg1)	3,8-4,9 % Cu; 1,2-1,8 % Mg; 0,3-0,9 Mn; ≤0,5 % Fe; ≤0,5 % Si; ≤0,1 % Ni; ≤0,30 Zn; ≤0,1 % Ti; the rest (basis) – Al
Copper alloys	
Technically pure copper M0	Basis – 99,95 % Cu, impurity - ≤0,05 %
Brass L63 (Cu63Zn37)	Basis – 62,0-65,0 % Cu; 34,5-37,5 % Zn; impurity - ≤0,5 %
Bronze BrA5 (Cu95Al5)	3,5-6 % Al; impurity - ≤0,5 %; the rest (basis) – Cu

To realize the EDI process the piece surface was processed in a sub-excitation regime, in which the processing occurs by "cold" electrode spots without surface layer melting of the processed material. The condition of the energy balance, in this case, takes the form [12]:

$$Q = \frac{4W_S}{\pi d_c^2 S} < Q_{melt}, \qquad (3)$$

where Q is the heat emitted on the surface of electrodes per volume unit, J/m^3; $W_S = \int_0^\tau u(t)i(t)dt$ is the energy emitted in the interstice, J; u(t) is the voltage on the interstice at the discharge, V; i(t) is the instantaneous value of the current in the interstice, A; τ is the duration of the discharge impulse, s; d_c is the diameter of the plasma canal, m; S is the distance between the electrodes (the interstice), m; $Q_{melt} = q_{melt} \cdot \rho_{melt}$ is the volumetric melting heat of the processed piece, J/m^3; q_{melt} is the specific melting heat of the processed piece, J/kg; ρ_{melt} is the material density at the temperature of melting, kg/m^3. So, for the EDI of construction steel, the energy emitted in the interstice of 1-2 mm will not exceed 6-10 J.

The impulse current generator [8, 9] with voltage block for interstice pre-ionization was used as a source of energy. The discharge energy emitted in the interstice constitutes 1-6 J. And, thus, establishing the generator energy regime, the superficial piece oxidation for indicated materials without melting of the processed surface can be produced.

The thickness of the oxide pellicle subjected to the condition of the energy balance and according to Palatnik's criterion [11], is directly proportional, respectively, to the quantity of heat and the energy emitted on the electrode surfaces:

$$\delta \sim Q; \quad \delta \sim W_S. \qquad (4)$$

The power of electrical discharge:

$$P = \frac{dW_S}{dt} = \frac{W_S}{\tau} \qquad (5)$$

where τ is duration of electrical discharge.

From the other point of view, the thickness of the oxide pellicle depends on the physical properties of processed surface material [5]:

$$\delta \sim \sqrt{\rho \cdot c \cdot \lambda}, \qquad (6)$$

where ρ is material density; c is specific thermal conductibility; λ is specific melting heat.

Thus, the thickness of the oxide pellicle is directly proportional to the power of electrical discharge emitted in the interstice and depends on the physical properties of processed surface material.

Technological schemes used in the formation of the oxide pellicles by applying EDI are shown in Fig. 1. The work-piece was connected in the discharge circuit as a cathode, and the tool-electrode – as an anode.

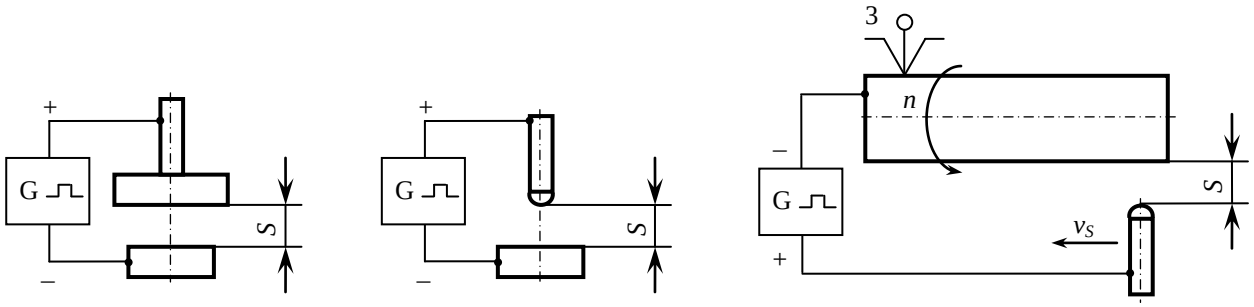

Fig. 1. Technological schemes of the oxide pellicle formation by applying EDI:
a) on the plane surface with plane tool-electrode; b) on the plane surface with a semi-circular tool-electrode; c) on the exterior cylindrical surfaces

The direct determination of operating properties that affect the functionality of pieces has required intensive investigations. Therefore, this task has been allocated for the performance that best suits the peculiarity of the work and does not require the use of lengthy and expensive techniques and equipment.

For evaluating and determining the operating properties of oxide coverings that characterize corrosion resistance, active surface resistance and other properties, the results of measuring the following characteristics of the coverings are presented: surface morphology (SEM), chemical (EDX) and phase (XPS) composition of coverings, the total pellicle thickness (Nanoscale Profilemeter).

3. RESULTS OF EXPERIMENTAL INVESTIGATIONS AND THEIR ANALYSIS

The results of SEM and EDX analysis of investigated sample surfaces are represented in Fig. 2-7 and in Table 2.

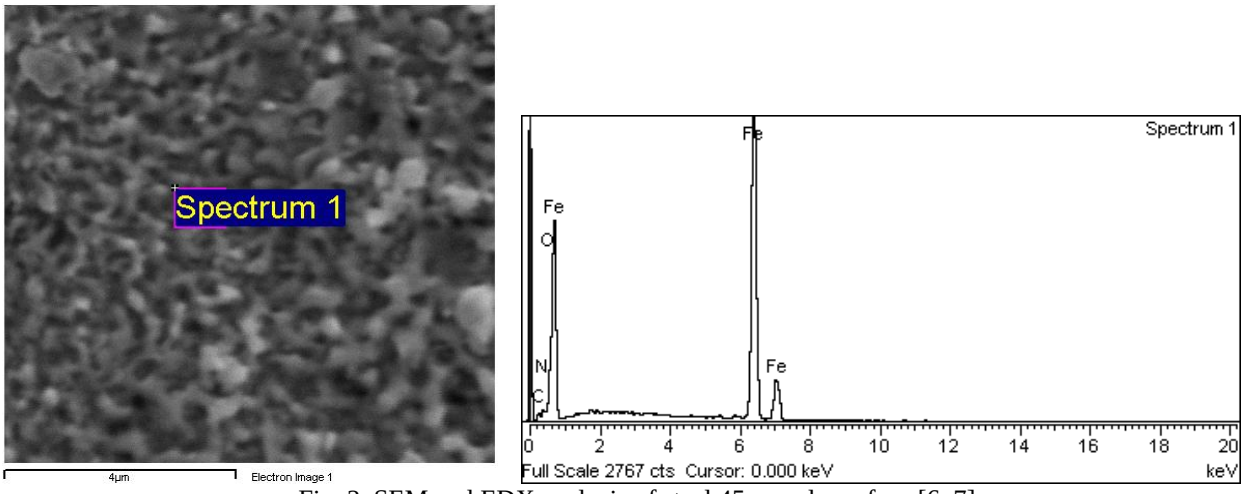

Fig. 2. SEM and EDX analysis of steel 45 sample surface [6, 7]

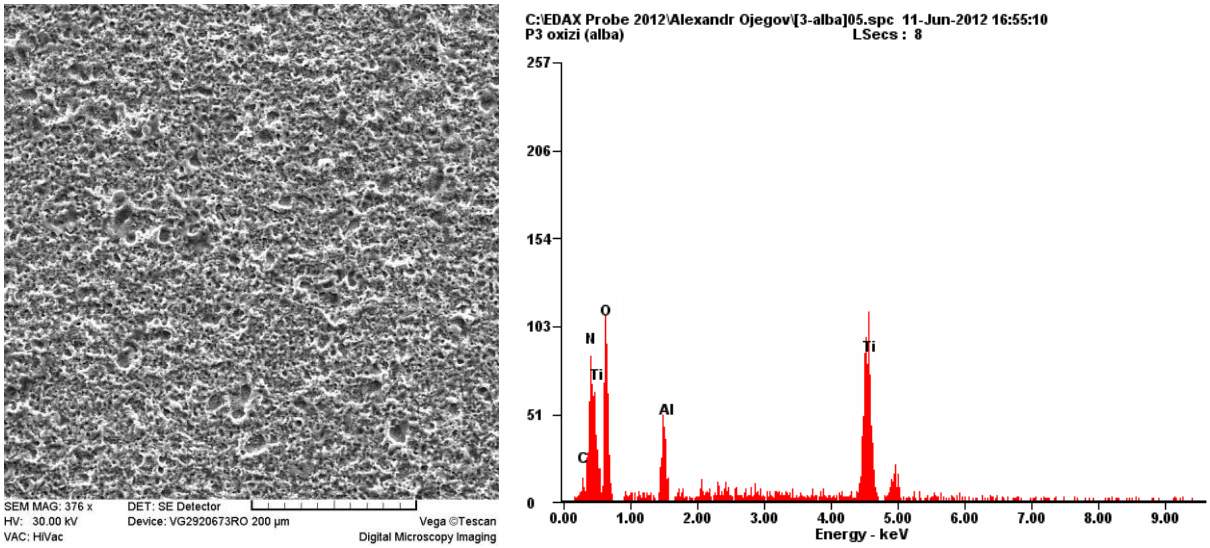

Fig. 3. SEM and EDX analysis of VT-8 titanium alloy sample surface

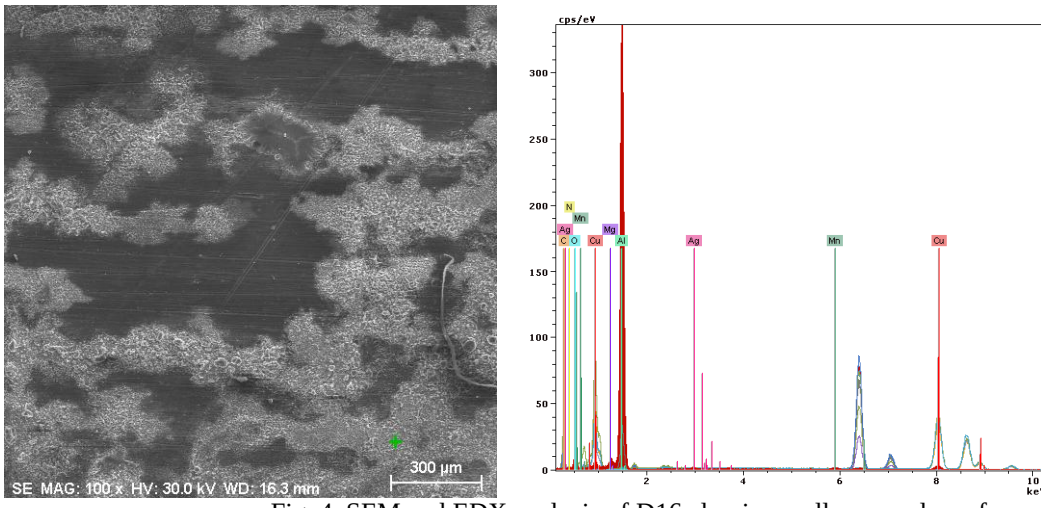

Fig. 4. SEM and EDX analysis of D16 aluminum alloy sample surface

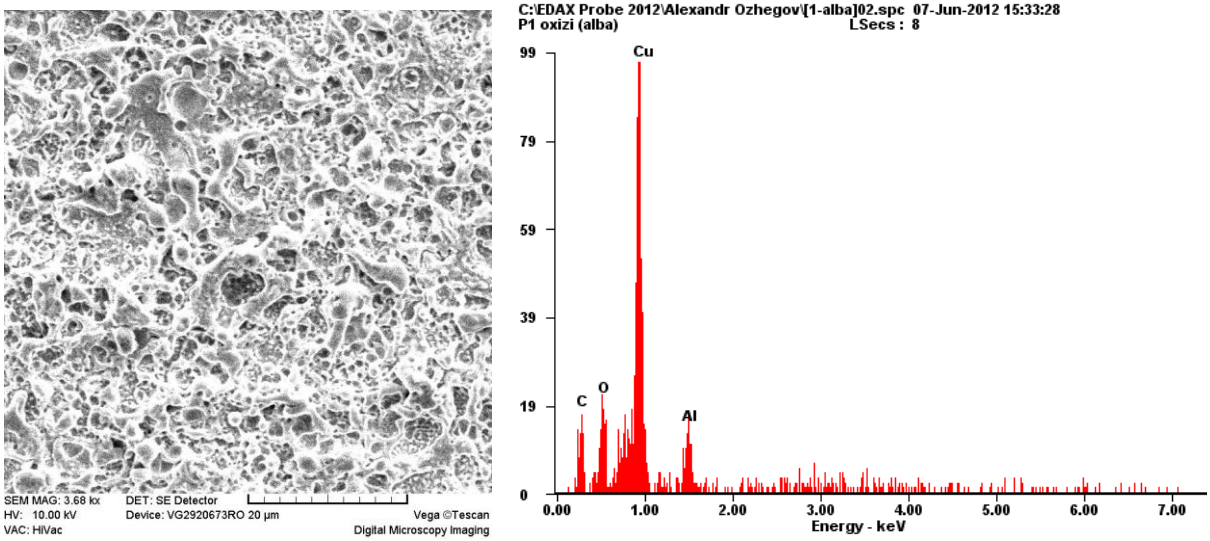

Fig. 5. SEM and EDX analysis of M0 copper alloy sample surface

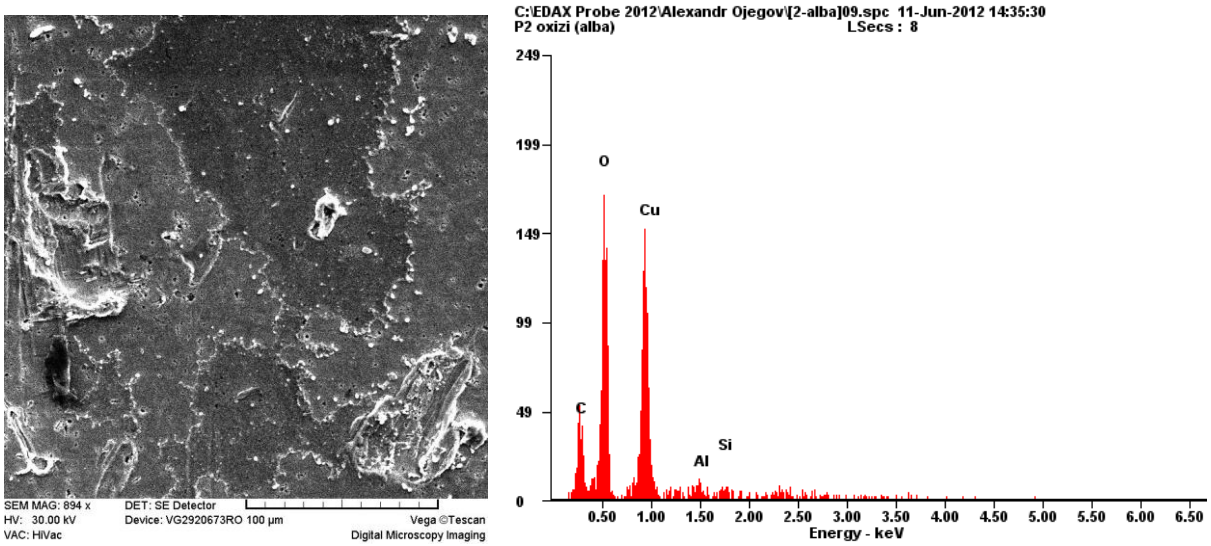

Fig. 6. SEM and EDX analysis brass L63 sample surface

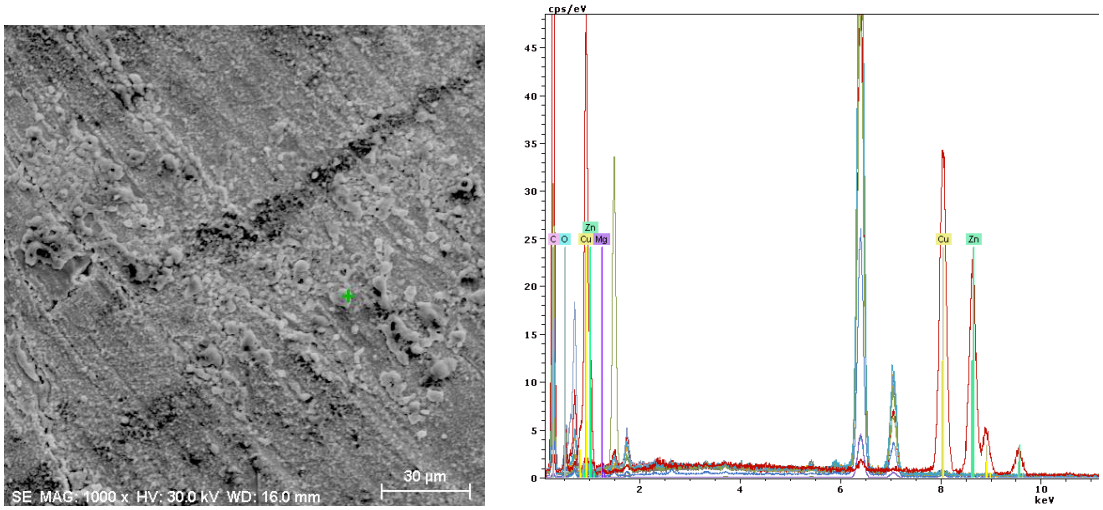

Fig. 7. SEM and EDX analysis bronze BrA5 sample surface

As we can see out of these results, the abnormal dissolving oxygen in metals is observed when processing metal surfaces by this method [6].

It is demonstrated that the desolation of the oxygen when processing the samples made of construction steel reaches 60% at, those made of titanium alloys – 30-35% at, the ones made of aluminum alloys – up to 20% at and those made of copper alloys – 50% at. The superficial layer of steel and titanium alloy surfaces includes, beside the oxygen, the nitrogen too.

Signal XPS analysis (Fig. 8) revealed the presence of oxygen O-1s in three types of chemical bonds (collectively called components).

These are: component O^{-2} (which contains oxygen atoms of the metal oxides, in the sample is labeled number 3 in Fig. 8, with the specific energy 529.6 EV); component OH^- with the specific energy 531.5 EV (indicated by the numeral 2 in Fig. 8); the relationship of O-C and O-C=O type (with the specific energy 533.4 EV, the curve no. 4 in Fig. 8).

The chemical analysis showed the concentration of each of the three components (C) (a): (C) (b): C (c) = 0.89: 1.00: 0.50. Additional studies have shown the possibility of the existence of the fourth component of oxygen within the context of type $O\text{-}H_2$, however, the relative concentration of the component value is assumed to be not greater than 0.15.

Table 2

The EDX analysis of sample element content

Basis material of the sample	EDX element content of processed surface		
	Element	[norm. wt.%]	[norm. at.%]
Steel 45 (C45)	Carbon	1.89	4.32
	Nitrogen	7.82	12.43
	Oxygen	29.77	58.74
	Iron	60.52	24.51
Titanium alloy VT-8 (TiAl6Mo4)	Carbon	00.41	01.38
	Oxygen	30.33	33.27
	Nitrogen	03.38	09.56
	Aluminum	05.84	08.57
	Titanium	60.04	47.22
Aluminum alloy D16 (AlCu4Mg1)	Aluminum	66.84	55.68
	Oxygen	13.95	19.60
	Magnesium	2.49	2.30
	Carbon	1.82	3.40
	Copper	2.42	0.86
	Manganese	0.55	0.23
	Silver	0.86	0.18
Technically pure copper M0	Copper	59.5	25.55
	Oxygen	29.53	50.50
	Carbon	10.22	23.20
	Aluminum	0.75	0.76
Bronze BrA5 (Cu95Al5)	Copper	52.97	21.18
	Oxygen	26.66	42.34
	Carbon	14.83	31.38
	Aluminum	02.66	02.50
	Silicate	02.87	02.60
Brass L63 (Cu63Zn37)	Copper	42.30	23.25
	Zinc	32.89	17.57
	Oxygen	16.72	36.50
	Carbon	7.52	21.86
	Magnesium	0.57	0.82

Studies have proven that when applying the EDI method for the formation of oxide pellicles there is no change in the geometry of the original surface.

This makes it possible for us to recommend this method for surface processing of completed parts. The thickness of films is between 10-240 nm [10], which allows us to include it at the level of nanotechnology.

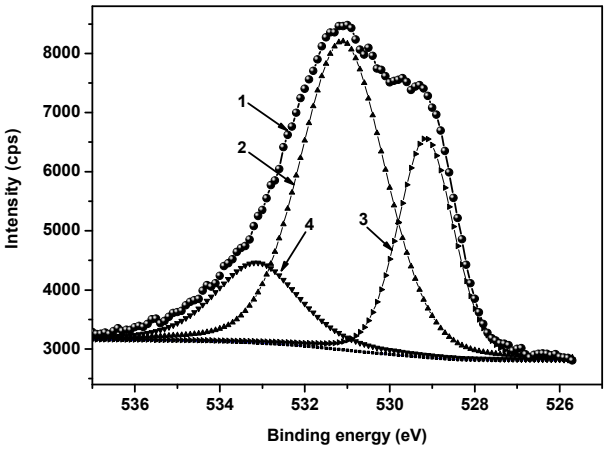

Fig. 8. The phase composition (by XPS analysis) of oxide pellicles on samples of steel 45 (spectrum of oxygen on the surface) [12]:
1 – total spectrum; 2 – OH^- component; 3 – O^{2-} component; 4 – components of O-C and O-C=O types

Oxides of metals in the pellicle are in amorphous state. This probably explains why the surface resistance for steel pieces increases up to 10^6 Ω/mm^2 [7], the potential to corrosion increases by 10 or more times, and the corrosion speed is reduced by 2...4 times [6, 7].

4. CONCLUSIONS

– the obtained results allow to recommend the ESO method for processing the internal and external surfaces of pieces made of iron, aluminum, copper and titanium alloys and to indicate the possibility of applying the method in anticorrosive protection of machine pieces, in surface passivation of pieces in the chemical industry;

– when processing the samples made of construction steel the desolation of the oxygen reaches 60% at, those made of titanium alloys constitutes 30-35% at, the ones made of aluminum alloys – up to 20% at and those made of copper alloys – 50% at.;

– XPS analysis of steel 45 samples' surfaces shows the presence of three types of oxygen components: OH^- component; O^{2-} component and the components of O-C and O-C=O types. The concentration of each of the three components is (C) (a): (C) (b): C (c) = 1.00: 0.89: 0.50;

– the superficial layer of steel and titanium alloy surfaces includes the nitrogen beside the oxygen;

– each compound formed while processing by electrical discharges in impulse is in amorphous non-stoichiometric state;

– maximal depth of oxide pellicles reaches up to 250 nm depending on energy regime and material of samples.

BIBLIOGRAPHY

1. Nemoshkalenko V.V., Topala P.A., Tomashevskii N.A., Mazanko V.F., Nosovskii O.I. Features of the formation of surface layers during spark discharges. Metal physics. Vol. 12, no. 3, May-June, 1990, p. 132-133.

2. Chernenko V.I. Snezhko L.A., Papanova I.I. Formation depositions by anodic-spark electrolysis. L., Chemistry, 1991. 128 p.

3. Gavrilov P.V., Lesnevskii L.N., Tverishin V.L., Tyurin V.N., Chernovskii M.N. Micro-ark oxidizing the work surfaces of the technological utensil elements made of aluminum alloys. Materials of the 9th international practical conference 10-13 April, 2007. Part. 2. Sent-Petersburg. Edition of Polytechnic Institute, 2007, p. 77-79.

4. Topala P.A., Ghitlevich A.E., Kornienko L.P. Corrosion properties of titanium with electro-spark alloying. Metal protection, Moscow, 1989, Vol. 29, No 3, p. 351-356.

5. Safronov I.I., Topala P.A., Gorbunov A.S. Electro-erosion processes on the electrodes and micro-structural and phase composition of alloying strata. Chisinau: TEHNICA-INFO, 2009. 495 p.

6. Topală P., Stoicev P., Ojegov A., Pînzaru N. Effects of abnormal dissolving of oxygen in metals under the influence of electrical discharges in impulse plasma. INTERNATIONAL JOURNAL OF MODERN MANUFACTURING TECHNOLOGIES, Vol. II (2) / 2010, p. 95-102.

7. Topala P., Stoicev P., Ojegov A., Pinzaru N., Monaico E. Analysis of processes occurring on the tool and piece electrode surface during the formation of oxide pellicles by applying electrical discharges in impulse. ModTech International Conference – New face of TMCR. 20-22 May 2010. Slanic-Moldova, Romania, p. 631-634.

8. Topala P., Ojegov A. Formation of oxide thin pellicles by means of electric discharges in pulse. Annals of the Oradea University. Fascicle of management and technological engineering, volume VII (XVII), 2008. CD-ROM Edition. Edition of the Oradea University, Romania, CNCSIS „Clasa B+”, p. 1824-1829.

9. Topala P., Ojegov A. Protection of internal cylindrical surfaces of the industrial pipes with oxide pellicles formed by applying electrical discharges in impulse. Agrarian State University of Moldova. Scientific papers. Vol. 21. Chisinau, 2008, p. 171-174.

10. Topala P., Stoicev P., Ojegov A. Experimental investigation on microoxidation of surfaces by means of applying electrical discharges in impulse under ordinary conditions. Creativity and Management. Proceedings of scientific papers. XIII Edition. Edition U.T.M., Chisinau, 2009, p. 172-175.

11. Nanu A., Nanu D. Dimensional processing by electrical erosion in the magnetic field. Edition FACLA, Timisoara, 1981, p. 15-32.

12. Topala P.A., Vizureanu P., Ojegov A.V., Stoicev P.N., Perju M.-K. Some results on micro-oxidation of metal surfaces by impulse discharges. Proceedings of the 13th International Scientific Conference "Technologies for repair, restoration and strengthening of machine parts, machinery, equipment, tools and tooling from nano- to macro-level", 12-15 April, 2011, Sankt-Petersburg, p. 1087-1094.

Prezentat la redacţie la 22 decembrie 2013

CZU XXX.XXX

EXIGENŢE PRIVIND PREZENTAREA LUCRĂRILOR ŞTIINŢIFICE PENTRU REVISTA „FIZICĂ ŞI TEHNICĂ: PROCESE, MODELE, EXPERIMENTE”

Nume_autor P.[1]*, Nume_autor P.[2], Nume_autor P.[n]
[1]Adresa completă a instituţiei primului autor
[2]Adresa completă a instituţiei autorului doi
[n]Adresa completă a instituţiei următorului autor
*e-mail: adresa e-mail a autorului pentru corespondenţă

Abstract: (max 10 lines) The sleep of reason produces monsters**,** the sleep of reason produces monsters**,** the sleep of reason produces monsters**,** the sleep of reason produces monsters**,** the sleep of reason produces monsters**,** the sleep of reason produces monsters**,** the sleep of reason produces monsters**,** the sleep of reason produces monsters**,** the sleep of reason produces monsters**,** Francisco José de Goya y Lucientes**.**

Keywords: (please, list 5-6 keywords).

Rezumat: **(maximum 10 rînduri)** Somnul raţiunii naşte monştri, somnul raţiunii naşte monştri, somnul raţiunii naşte monştri, somnul raţiunii naşte monştri, somnul raţiunii naşte monştri, somnul raţiunii naşte monştri, somnul raţiunii naşte monştri, somnul raţiunii naşte monştri, somnul raţiunii naşte monştri, somnul raţiunii naşte monştri, somnul raţiunii naşte monştri, somnul raţiunii naşte monştri, somnul raţiunii naşte monştri, Francisco José de Goya y Lucientes**.**

Cuvinte-cheie: (introduceţi 5-6 cuvinte-cheie).

I. DESTINAŢIA REVISTEI

Materialele prezentate în revistă vor reflecta realizările obţinute în ultimii ani în cadrul catedrelor, laboratoarelor de cercetări ştiinţifice ale USARB, instituţiilor de învăţământ şi de cercetare din Republica Moldova şi de peste hotarele ei.

În revistă se publică articole ştiinţifice ce ţin de următoarele domenii de cercetare:

- propagarea undelor de radio în diverse medii;
- elaborarea dispozitivelor electronice analogico-numerice;
- elaborarea laserilor şi aplicarea lor în tehnologiile de prelucrare a materialelor;
- studierea infleunţei factorilor exteriori asupra proprietăţilor fizice ale substanţei;
- tehnologii clasice şi neconvenţionale de prelucrare a materialelor.

II. CERINŢE FAŢĂ DE ARTICOLELE PREZENTATE

2.1. Dispoziţii generale

Nu se vor admite pentru publicare materiale care au fost publicate în alte ediţii. Articolele vor fi însoţite de extrasul din procesul verbal al şedinţei de catedră, al laboratorului sau seminarului ştiinţific la care au fost discutate şi propuse pentru publicare. Lucrările primite la redacţie vor fi recenzate de specialişti calificaţi în domeniul respectiv, numiţi de colegiul de redacţie.

2.2. Structura lucrărilor şi regulile de prezentare

O persoană poate fi autor sau/şi coautor la maximum două articole. Volumul unui articol nu va depăşi, ca regulă, 7 pagini.

Fiecare articol va cuprinde:

- CZU;
- titlul în limbile originalului, română şi engleză;
- date despre autor/autori în limbă română şi engleză;
- rezumatul în limbile originalului, română şi engleză;
- cuvinte-cheie;
- articolul propriu-zis;
- bibliografie.

2.3. Întrebuinţarea suportului electronic

Materialele vor fi redactate în **Microsoft Word,** fontul **Times New Roman** şi vor fi prezentate pe foi în formatul A4

(297X210 mm). Parametrii paginii: 25 - stînga (Left), 20 - sus (Top), 20 - jos (Bottom), 15 - dreapta (Right), 12,5 - antet (Header), 0 - subantet (Footer), 2 coloane. Dimensiunile fontului de imprimare - 12 points. Aliniatele – 1 cm. Spaţiul dintre liniile (Line Spacing) aceluiaşi paragraf, inclusiv titlul lucrării şi informaţiile despre autori - un interval. Se va accepta cu trecerea cuvintelor dintr-un rînd în altul. Ultima pagină, în limita posibilităţilor, va fi completă.

2.4. Structura articolului

CZU se va situa în partea stîngă a paginii.

Titlul se va da complet, maximum 3 rînduri, pe toată lăţimea paginii (12 points, BOLD, CENTER, ALL CAPS).

Informaţiile despre autori se vor da cu aldine, în limba în care este scrisă lucrarea, în următoarea consecutivitate: Numele şi Prenumele autorului, afilierea. Dacă coautorii lucrării sînt angajaţii aceleiaşi instituţii, denumirea ei se va da o singură dată. Pentru corespondenţa se indică e-mail-ul unuia din autori, însemnat cu asterix.

Rezumatul va cuprinde descrierea succintă a obiectului, metodelor şi rezultatelor cercetării în limbile română şi engleză şi nu va depăşi 10 rînduri. Mărimea caracterilor – 10 points. Cuvîntul „Rezumat” nu se va indica.

Cuvintele-cheie vor fi indicate după rezumatul articolului în limbile originalului, română şi engleză.

*Introducere*a va reflecta stadiul actual al cercetărilor în domeniu. În caz de necesitate, va cuprinde o scurtă analiză istorică. Introducerea se va încheia cu expunerea scopului lucrării.

Conţinutul lucrării va include expunerea metodicii cercetării (experimentală sau teoretică), obiectul cercetării, echipamentul, metodele de măsurare şi de observare, precizia şi erorile metodicii experimentului. Se vor indica rezultatele obţinute şi analiza lor. Nu se va admite repetarea datelor în tabele, desene şi texte.

În concluzii se va expune succint esenţa cercetării efectuate, relievîndu-se importanţa şi gradul de noutate a rezultatelor obţinute.

Titlul fiecărui paragraf se va evidenţia cu aldine. Titlurile de capitol vor fi separate de textul curent printr-un spaţiu.

În faţa textului fiecare titlu de subcapitol cu doi indici se lasă un spaţiu liber de un rînd. Aliniatele se vor marca prin introducerea unui „‹Tab›”. Pentru scoaterea în relief a unor concepte se vor folosi aldinele **(fără subliniere).**

Tabele se vor numerota cu cifre arabe în partea stîngă (de ex.: „Tabelul 1”), după care, în acelaşi rînd, va urma denumirea şi tabelul propriu-zis. Tabelele vor fi separate de textul curent printr-un spaţiu. Toate liniile ce formează coroiajul tabelului vor avea aceeaşi grosime (1 points). În tabela textuală cifrele se vor scrie cu fontul 10 points, normal. Dacă textul va conţine un singur tabel, acesta nu se va numerota.

Ilustraţiile (figurile, schemele, diagramele, fotografiile etc.) se vor prezintă în alb-negru, inserate în textul de bază sau pe foi aparte. Toate figurile se vor numerota cu cifre arabe (în ordinea apariţiei lor în lucrare), după care se va da legenda lor. Toate semnele sau marcările ilustrate se vor defini în legendă. În cazul mărimilor fizice, se vor indica unităţile de măsură. Dacă lucrarea va conţine o singură figură, ea nu se va numerota. Figurile vor fi separate de textul curent printr-un spaţiu. Fotografiile introduse în text se vor scana cu o rezoluţie de minim 300 dpi (preferabil 600 dpi) şi se vor prelucra pentru un contrast bun.

Nu se admite lipirea fotografiilor sau desenelor pe foi separate. Adnotările de pe figuri se vor face în cifre sau litere cu înălţimea caracterelor echivalentă fontului 10 points. Legenda se va culege cu 10 points.

Formule matematice. Toate formulele matematice se vor scrie, **ÎN MOD OBLIGATORIU,** cu editorul de ecuaţii din procesorul de texte Microsoft Word for Windows'95/, 97/, 98/, 2000, (Version 6.0/,Version 7.0, 2000) italice, centrat, prin culegerea fiecăreia din rînd nou. Exigenţele corespunzătoare vor urma imediat după formulă şi se vor întroduce prin „unde”, respectîndu-se ordinea semnelor din ecuaţie sau relaţie. Dacă textul va conţine mai multe ecuaţii sau relaţii, acestea se vor numerota cu cifre arabe la sfîrţitul rîndului, în partea dreaptă a coloanei. După descifrarea simbolului-literă, se va pune virgula, apoi se va indică unitatea de măsură.

Unităţile de măsură ale mărimilor fizice se vor prezenta în sistemul internaţional de unităţi (SI).

Bibliografia Termenul „Bibliografie” va fi separat de textul curent prin spaţiu. În text, referinţele se vor insera prin cifre încadrate între croşete, de exemplu: [2], [5-7], şi se vor prezenta la sfîrşitul articolului într-o listă aparte, în ordinea apariţiei lor în text, în conformitate cu cerinţele CNAA al Republicii Moldova. Referinţele bibliografice se vor da în limba originalului. Nu se vor accepta referinţe la surse nepublicate.

III. OBSERVAŢII FINALE

Informaţia despre autori şi rezumatele în alte limbi decît originalul se vor plasa după bibliografie. Conţinutul rezumatului expus în trei limbi va fi identic.

Materialul cules se va prezenta în format electronic prin e-mail la adresa secretarului ştiinţific (alexandr.ozhegov@yahoo.com) sau la adresa redactorului-şef al revistei (pavel.topala@gmail.com), precum şi într-un exemplar printat (cu contrastul bun) semnat de toţi autorii (după bibliografie).

Pentru relaţii suplimentare se va indica adresa, numărul de telefon şi e-mail-ul unuia dintre autori.

Articolele care nu vor corespunde cerinţelor expuse, normelor limbii şi stilului vor fi respinse.

Materialele prezentate la redacţie nu se vor restitui autorului.

Prezentat la redacţie la DD MMMM YYYY

UDC XXX.XXX

GUIDELINES FOR SUBMISSION OF SCIENTIFIC PAPERS TO THE JOURNAL „PHYSICS AND TECHNICS: PROCESSES, MODELS, EXPERIMENTS”

Name_author P.[1]*, Name_author P.[2], Name_author P.[n]
[1]Full address of the first author's institution
[2]Full address of the second author's institution
[n]Full address of the next author's institution
*e-mail: adresa e-mail a autorului pentru corespondenţă

Abstract: (max 10 lines) The sleep of reason produces monsters**,** the sleep of reason produces monsters**,** the sleep of reason produces monsters**,** the sleep of reason produces monsters**,** the sleep of reason produces monsters**,** the sleep of reason produces monsters**,** the sleep of reason produces monsters**,** the sleep of reason produces monsters**,** the sleep of reason produces monsters**,** Francisco José de Goya y Lucientes**.**

Keywords: (please, list 5-6 keywords).

Rezumat: **(maximum 10 rînduri)** Somnul raţiunii naşte monştri, somnul raţiunii naşte monştri, somnul raţiunii naşte monştri, somnul raţiunii naşte monştri, somnul raţiunii naşte monştri, somnul raţiunii naşte monştri, somnul raţiunii naşte monştri, somnul raţiunii naşte monştri, somnul raţiunii naşte monştri, somnul raţiunii naşte monştri, somnul raţiunii naşte monştri, somnul raţiunii naşte monştri, somnul raţiunii naşte monştri, Francisco José de Goya y Lucientes**.**

Cuvinte-cheie: (introduceţi 5-6 cuvinte-cheie).

I. THE JOURNAL SCOPE

The submitted materials should reflect recent achievements of the Alecu Russo Balti Sate University departments and research laboratories and of educational and research institutions from the Republic of Moldova and abroad.

The journal publishes scientific articles related to the following research areas:
- radio wave propagation in various media;
- development of numerically-analogical electronic devices;
- development of lasers and their application in material processing technologies;
- the study of external factor influence on the physical properties of the substance;
- classical and non-conventional technologies of material processing.

II. REQUIREMENTS FOR ARTICLE SUBMISSION

2.1. General arrangements

Papers that have been published in other editions are not accepted. Articles should be accompanied by an extract from the minutes of the Chair/Laboratory/Scientific Seminar sitting where the papers had been discussed and recommended for publication. The submitted papers should be subject to the review of qualified specialists in the field, appointed by the editorial board.

2.2. Paper format and rules for submission

A person may be the author and / or coauthor of at most two articles. The volume of an article should not exceed, as a rule, 7 pages. Each article should include:
- UDC;
- the title in original language, Romanian and English;
- information about the author/authors in original language, Romanian and English;
- the abstract in Romanian and English;
- the keywords in Romanian and English;
- the article itself;
- the bibliography.

2.3. Use of electronic support

Materials should be edited in **Microsoft Word**, **Times New Roman** font and page size should be A4 (297X210 mm). Page parameters: 25 - Left, 20 - Top, 20 - Bottom, 15 - Right, 12.5 - Header, 0 - Footer, 2

columns. Font size Print - 12 points. Paragraphs - 1 cm. Line Spacing within the same paragraph including the title and information about the author – one interval. Transference of words from one line to another is accepted. It is desirable that the last page should be complete.

2.4. Structure of the article

UDC should be placed on the left side of the page.

The title should be complete, up to 3 lines, on the full width of the page (12 points, BOLD, CENTER, ALL CAPS).

The information about the authors should be given in bold in the language of the written paper in the following sequence: author's surname and first name (full), affiliation. If the co-authors are employees at the same institution, its name should be given only once.

The abstract should include a brief description of the subject matter, methods and research findings and should not exceed 10 lines. Font size - 10 points. The word "Abstract" should not be typed.

The keywords will be listed after the abstract in original language, Romanian and English.

The introduction should reflect the current state of research in the field. If need be, it will include a brief historical analysis. The introduction should end with an account of the paper aims.

The main text should include an account of the research methodology (experimental or theoretical), subject of research, equipment, measurement and observation methods, the precision and errors of the experiment methodology. It should include the results and their analysis. It is not allowed to repeat data in tables, drawings and texts.

The conclusion should briefly expound on the essence of conducted research highlighting the importance and degree of the novelty of results.

The title of each paragraph should be in bold. A space should be left between chapter titles and the text.

One line space is left before the text of each two index sub-chapter title. Paragraphs should be marked by the introduction of a "<Tab>". Bold type (no underlying) should be used to emphasize certain concepts.

The tables should be numbered with Arabic numerals on the left (e.g.: "Table 1"); this should be followed in the same line by the title and the table itself. The tables should be separated from the current text by one space. All the lines that form the table welding should have the same thickness (1 point). The font of the figures in the text of the table should be normal, 10 points. If the text contains a single table, it should not be numbered.

The illustrations (figures, charts, diagrams, photos, etc...) should be black and white, inserted in the main text or on separate sheets. All figures should be numbered with Arabic numerals (in order of their appearance in the paper) after which they should be explained. All signs and markings should be defined in the explanatory text. If there are physical dimensions, the measurement units should be indicated. In case the work contains only one figure it should not be numbered. The figures should be separated from the current text by a space. The photographs included in the text should be scanned at a minimum of 300 dpi (preferably 600 dpi) resolution and should be processed for a good contrast.

It is not allowed to stick photos or drawings on separate sheets. The notes on figures should be in numbers or letters with similar 10 point font characters. The explanatory text should be typed with the same character size - 10 points.

Mathematical formulas. **It is obligatory** to write all mathematical formulas using the equation editor of Microsoft Word processor for Windows 95/97/98/2000, (Version 6.0 /, Version 7.0, 2000) in italics, centered, each one should be typed beginning with a new line. The corresponding requirements should immediately follow the formula beginning with "where" and observing the order of signs in the equation or relation. If the text contains more equations or relations, they should be numbered with Arabic numerals at the end of the line on the right side of the column. A comma should be used after the letter - symbol is deciphered; the measurement unit should be indicated.

The measurement units of physical dimensions should be presented through the International System of Units (SI).

The bibliography. The term "*Bibliography*" should be separated from the text by space. In the text, the references should be inserted by numbers enclosed in square brackets, e.g. [2], [5-7], and should come at the end of the article in a separate list in order of their appearance in the text, in concordance with requirements submitted by NCAA of the Republic of Moldova. The references should be given in the source language. References to unpublished sources are not allowed.

III. CONCLUDING REMARKS

The information about authors and the abstracts in languages other than the source one should be placed after the bibliography. The content of the abstract presented in three languages should be identical.

The typed material should be presented both in electronic format send by e-mail (on the scientific secretary address alexandr.ozhegov@yahoo.com or on the responsible editor's address pavel.topala@gmail.com) and in a printed copy (with good contrast) signed by all authors (after the Bibliography).

One of the authors' address, telephone number and E-mail should be indicated for additional information.

The articles that do not meet the described requirements, the norms of language and style will be rejected.

The materials submitted to the editorial board will not be returned to the author.

Prezentat la redacţie la DD MMMM YYYY

Bun de tipar 20.08.2015. Garnitura Times New Roman. Comanda nr. 4. Tiraj 100.
Tipografia Indigou Color, m Bălţi, str. Puşkin, 38